RESEARCH ARTICLE

WILEY

Resting-state functional connectivity of the human hippocampus in periadolescent children: Associations with age and memory performance

David E. Warren[1] ⬤ | Anthony J. Rangel[1] | Nicholas J. Christopher-Hayes[1] |
Jacob A. Eastman[1] | Michaela R. Frenzel[1] | Julia M. Stephen[2] |
Vince D. Calhoun[2,3] | Yu-Ping Wang[4] | Tony W. Wilson[1,5] ⬤

[1]Department of Neurological Sciences, University of Nebraska Medical Center, Omaha, Nebraska

[2]The Mind Research Network, Albuquerque, New Mexico

[3]Tri-institutional Center for Translational Research in Neuroimaging and Data Science (TReNDS), Georgia State University, Georgia Institute of Technology, Emory University, Atlanta, Georgia

[4]Tulane University, New Orleans, Louisiana

[5]Boys Town National Research Hospital, Boys Town, Nebraska

Correspondence
David E. Warren, Department of Neurological Sciences, University of Nebraska Medical Center, Omaha, NE.
Email: david.warren@unmc.edu

Abstract

The hippocampus is necessary for declarative (relational) memory, and the ability to form hippocampal-dependent memories develops through late adolescence. This developmental trajectory of hippocampal-dependent memory could reflect maturation of intrinsic functional brain networks, but resting-state functional connectivity (rs-FC) of the human hippocampus is not well-characterized for periadolescent children. Measuring hippocampal rs-FC in periadolescence would thus fill a gap, and testing covariance of hippocampal rs-FC with age and memory could inform theories of cognitive development. Here, we studied hippocampal rs-FC in a cross-sectional sample of healthy children ($N = 96$; 59 F; age 9–15 years) using a seed-based approach, and linked these data with NIH Toolbox measures, the Picture-Sequence Memory Test (PSMT) and the List Sorting Working Memory Test (LSWMT). The PSMT was expected to rely more on hippocampal-dependent memory than the LSWMT. We observed hippocampal rs-FC with an extensive brain network including temporal, parietal, and frontal regions. This pattern was consistent with prior work measuring hippocampal rs-FC in younger and older samples. We also observed novel, regionally specific variation in hippocampal rs-FC with age and hippocampal-dependent memory but not working memory. Evidence consistent with these findings was observed in a second, validation dataset of similar-age healthy children drawn from the Philadelphia Neurodevelopment Cohort. Further, a cross-dataset analysis suggested generalizable properties of hippocampal rs-FC and covariance with age and memory. Our findings connect prior work by describing hippocampal rs-FC and covariance with age and memory in typically developing periadolescent children, and our observations suggest a developmental trajectory for brain networks that support hippocampal-dependent memory.

KEYWORDS
adolescence, development, hippocampus, memory, resting-state functional connectivity

1 | INTRODUCTION

The hippocampus is necessary for normal declarative (relational) memory (Cohen & Squire, 1980; Eichenbaum & Cohen, 2001; Scoville & Milner, 1957), and the ability to form hippocampal-dependent memories develops throughout early life (Ghetti & Bunge, 2012; Ofen, 2012). Specifically, hippocampal-dependent memory abilities improve significantly from early childhood through middle childhood and adolescence (Lee, Wendelken, Bunge, & Ghetti, 2016; Overman, Pate, Moore, & Peuster, 1996) reaching maturity in early adulthood (DeMaster, Pathman, Lee, & Ghetti, 2014; Finn et al., 2016; Ghetti, DeMaster, Yonelinas, & Bunge, 2010; Ofen et al., 2007; Sowell, Delis, Stiles, & Jernigan, 2001). Consistent with findings of dissociable memory abilities in studies of adults (Cohen & Squire, 1980; Eichenbaum & Cohen, 2001; Scoville & Milner, 1957), the developmental trajectory of memory abilities (including hippocampal-dependent memory) does not appear to reflect changes in a unitary memory system or factor (Brainerd, Stein, & Reyna, 1998; Finn et al., 2016; Schneider, Bjorklund, & Valsiner, 2003). Rather, hippocampal-dependent memory abilities likely represent one of a set of memory processes with relatively independent developmental courses, functions, and brain correlates (Finn et al., 2016; Olson & Newcombe, 2014; Schneider et al., 2003). Regarding the development of those brain correlates, the age-related trajectory of hippocampal-dependent memory suggests that functional properties of the hippocampus and related brain networks change during childhood. While the intrinsic functional connectivity of the hippocampus has been studied in early-to-middle childhood (Blankenship, Redcay, Dougherty, & Riggins, 2017) and young adults (Kahn, Andrews-Hanna, Vincent, Snyder, & Buckner, 2008; Vincent et al., 2006), periadolescent age-related differences in the intrinsic functional connectivity of the hippocampus—and the impact of these differences on associated cognitive abilities—are not well characterized (Ghetti & Bunge, 2012).

Measuring periadolescent changes in brain networks is important because adolescence marks the last epoch of substantial cognitive and brain development prior to the relative stability of early adulthood (Dahl, 2004; Faghiri, Stephen, Wang, Wilson, & Calhoun, 2017; Fair et al., 2008; Giedd, 2008; Lenroot & Giedd, 2006; Stevens, Pearlson, & Calhoun, 2009). Concretely, periadolescent cognitive development has been hypothesized to rely on increased segregation between functional brain networks coupled with increased integration within those networks (Fair et al., 2008; Johnson, 2001; Menon, 2013; Stevens et al., 2009). This putative trajectory means that adolescence may present unique opportunities for identifying brain-network measures related to developmental status (Nielsen et al., 2019) as well as for discriminating healthy normal development from neurological or psychiatric disease (Lenroot & Giedd, 2006; Uddin, Supekar, & Menon, 2010; Volkow et al., 2018). The hippocampus could have special relevance for the latter because the structure is vulnerable to many disease processes (e.g., epilepsy, depression, schizophrenia, and, in old age, Alzheimer's disease) (Hare et al., 2018; Joëls, 2009; Mac-Master & Kusumakar, 2004; Mohamed et al., 2001; van Erp et al., 2016; Zhou et al., 2008) and detrimental environmental

influences (e.g., stress, trauma, and prenatal alcohol exposure) (Carrion, Weems, & Reiss, 2007; Hanson et al., 2015; Jackowski, de Araújo, de Lacerda, de Jesus, & Kaufman, 2009; Uecker & Nadel, 1996). These vulnerabilities further motivate the study of healthy normal hippocampal development—including its intrinsic functional connectivity—with the goal of beginning to establish normative expectations for adolescent variation. Notably, evaluating hippocampal intrinsic functional connectivity as a relevant, valid biomarker for disease in adolescent populations would be beyond the scope of a single study. However, the broader potential of intrinsic functional brain network measures as biomarkers has been discussed extensively (Damoiseaux, 2012; Hohenfeld, Werner, & Reetz, 2018; Zhang & Raichle, 2010) albeit with important caveats regarding the reliability of and approach to measuring resting-state functional connectivity (rs-FC; Ciric et al., 2017; Noble, Scheinost, & Constable, 2019).

The intrinsic functional connectivity of the hippocampus has been studied with resting-state functional MRI (rs-fMRI) in populations including early-to-middle childhood (age 4–10 years) (Blankenship et al., 2017) and healthy young adults (age 19–35 years) (Kahn et al., 2008; Vincent et al., 2006). These reports describe a widespread network of brain regions functionally coactive with the hippocampus including posterior cingulate, ventromedial prefrontal cortex, and angular gyrus (among others). Further, there appears to be some regional specificity within this hippocampal network as anterior and posterior hippocampal regions (and adjacent medial temporal lobe neocortex) show moderate differences in their patterns of functional connectivity (Blankenship et al., 2017; Hrybouski et al., 2019; Kahn et al., 2008; Poppenk & Moscovitch, 2011; Qin et al., 2016; Ranganath & Ritchey, 2012; Riggins, Geng, Blankenship, & Redcay, 2016; Tang et al., 2020). Beyond the importance of these findings as novel empirical observations, evidence of an anterior–posterior gradient in hippocampal functional connectivity shows that new studies in this domain should address intrahippocampal variation in functional connectivity whether as a primary focus or as necessary consideration when studying whole-hippocampus functional connectivity and related brain networks.

The set of brain regions exhibiting intrinsic functional connectivity with the hippocampus strongly resembles a well-characterized, large-scale intrinsic network—the default mode network (DMN) (Biswal, Zerrin Yetkin, Haughton, & Hyde, 1995; Raichle et al., 2001). Conversely, descriptions of DMN extent often include hippocampus as a component (Andrews-Hanna et al., 2007; Buckner, Andrews-Hanna, & Schacter, 2008; Ward et al., 2014). Studies of the DMN from middle childhood through early adulthood have revealed robust developmental effects (Chai, Ofen, Gabrieli, & Whitfield-Gabrieli, 2014a; Fair et al., 2008; Supekar et al., 2010), and regional patterns of anticorrelation with the DMN (Fox et al., 2005; Fox, Zhang, Snyder, & Raichle, 2009) may also change during development (Barber, Caffo, Pekar, & Mostofsky, 2013; Chai et al., 2014a). Specifically, adults often exhibit greater positive connectivity than children between the medial prefrontal cortex and other DMN components (Barber et al., 2013; Supekar et al., 2010) but greater negative connectivity between DMN and regions such as dorsolateral prefrontal cortex,

superior parietal lobule, or insula (Barber et al., 2013; Chai et al., 2014a). Hippocampal functional connectivity could follow a similar trajectory, and in young children (4–10 years), age-related changes in whole-hippocampus functional connectivity have been identified in middle temporal gyrus, superior temporal gyrus, and piriform cortex (Blankenship et al., 2017). However, age-related changes in hippocampal functional connectivity have not been described for the periadolescent epoch (i.e., late middle childhood through early adolescence, age 9–15).

Functional differences in the developing hippocampus and a connected network of brain regions may also contribute to individual differences in memory performance. Analysis of hippocampal rs-FC in children aged 4–8 years showed that episodic memory ability covaried with hippocampal rs-FC in specific brain regions (ventromedial prefrontal cortex, precuneus, and middle temporal gyrus) (Geng, Redcay, & Riggins, 2019; Riggins et al., 2016). Further, regionally specific associations between memory ability and hippocampal rs-FC have also been reported in healthy older adults (in left inferior parietal lobule, posterior cingulate, and medial prefrontal cortex) (Wang et al., 2010). Meanwhile, healthy young adults exhibit a functional network topology in inferior parietal lobule—which reliably shows rs-FC with the hippocampus—associated with memory retrieval processes (Nelson et al., 2010; Vincent et al., 2006). These findings suggest an intrinsic organization of the hippocampus and other brain regions associated with memory ability. Consistent with this, the hippocampus and a network of brain regions are implicated in active memory processes by task-based fMRI studies (Geng et al., 2019; Kim, 2011; Spreng, Mar, & Kim, 2009; Svoboda, McKinnon, & Levine, 2006). Periadolescent memory ability may therefore be related to the intrinsic organization of a functional network that includes the hippocampus.

In the current study, we used a cross-sectional design to measure the intrinsic functional connectivity of the hippocampus with the whole brain in a periadolescent youth sample aged 9–15 years old ($N = 96$) using resting-state functional MRI (rs-fMRI) data measured with a seed-based approach. A secondary objective was to test whether the pattern of rs-FC covaried with participants' age and memory performance. Memory performance was measured in two domains using tests from the NIH Toolbox (Weintraub et al., 2013): for relational memory, the Picture Sequence Memory Test (PSMT; Dikmen et al., 2014) was predicted to rely heavily on hippocampus-dependent relational processing (Eichenbaum & Cohen, 2001; Ranganath, 2010) even during the short testing interval (Gazzaley, Rissman, & D'Esposito, 2004; Hannula, Tranel, & Cohen, 2006; Hannula, Ryan, Tranel, & Cohen, 2007; Ranganath & D'Esposito, 2001; Warren, Duff, Jensen, Tranel, & Cohen, 2012; Watson, Voss, Warren, Tranel, & Cohen, 2013); and for working memory, the List Sorting Working Memory Test (LSWMT; Tulsky et al., 2014) which was not predicted to rely heavily on hippocampus-dependent processing. Based on prior reports describing younger and older samples (Blankenship et al., 2017; Kahn et al., 2008; Vincent et al., 2006), we predicted that the overall pattern of hippocampal rs-FC would show strong positive connectivity with neighboring medial temporal lobe regions and a broader network of regions in prefrontal, temporal, cingulate, and parietal association cortex. Further, we predicted that

age and memory performance would be linked to unique local modulations of hippocampal rs-FC with frontal, temporal, insular, and/or parietal regions (Blankenship et al., 2017; Geng et al., 2019; Riggins et al., 2016; Wang et al., 2010). Our approach incorporated important control measures including analysis of any influence of global signal. We also measured and contrasted anterior and posterior hippocampal rs-FC. Finally, we evaluated the generalizability of our findings from the first, discovery dataset by applying the same processing and analysis approach to a second, validation dataset, initially in isolation and then in an analysis that combined second-level analyses from the discovery and validation datasets.

2 | METHODS

We used two datasets in this study, the first for discovery and the second for validation. The primary, discovery dataset was drawn from the Developmental Chronnecto-Genomics (Dev-CoG) project (see next sections). The validation dataset was a subset of the Philadelphia Neurodevelopmental Cohort (Satterthwaite et al., 2016) (see Section 2.6). We analyzed the discovery and validation datasets separately, and then together in a combined analysis using a meta-analytic approach.

2.1 | Participants

Participants were healthy normal children age 9–15 years who were enrolled in the Dev-CoG project (Stephen et al., 2021). Inclusion criteria for the current study were: no incidental findings on MRI; structural MRI data of sufficient quality to allow automated segmentation with FreeSurfer (Fischl, 2004) and manual tracing of the hippocampus bilaterally; rs-fMRI data with a sufficient number of low-motion volumes to support preprocessing and analysis (see MRI data processing section 2.4.); and scores on two NIH Toolbox measures (see next section). These criteria yielded a sample of $N = 96$ children (59 females, 37 males) with ages ranging from 9.1 to 15.1 years (mean = 12.1, $SD = 1.7$) (Figure 1). Otherwise eligible participant datasets that were excluded due to insufficient fMRI data after censoring for excessive motion equaled 58; each excluded dataset had at
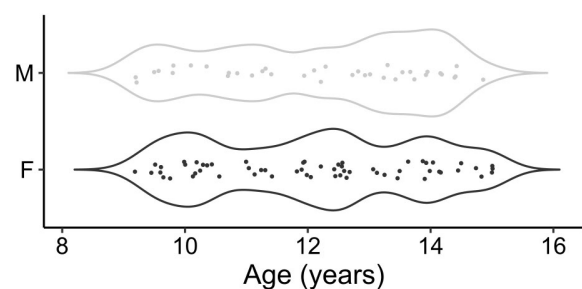
FIGURE 1 Participant age in the discovery dataset ranged from 9 to 15 years and was evenly distributed in the whole sample and within sex. Points represent individual participant age and sex (gray, male; black, female); lines indicate density of observations across age

least 71 fMRI volumes censored (mean censored volumes = 192; mean maximum framewise displacement [FD] = 1.45 mm).

The sample contained significantly more females than would be expected by chance (binomial test vs. 0.5, p = .032), but there were no differences in age between sexes ($T(94)$ = 0.174, p = .862). The sample was evenly divided between two data collection sites with 48 datasets collected per site (see Section 2.3.1). Parents or legal guardians of each participating child gave written informed consent prior to participation, and children gave assent. All procedures were approved by the institutional review board of the University of Nebraska Medical Center (UNMC) and Chesapeake IRB for the Mind Research Network site, and the study protocol was conducted in a manner consistent with the principles of human subjects research described in the Declaration of Helsinki.

2.2 | Behavioral measures

2.2.1 | Tasks

Participants used an Apple iPad to complete a battery of NIH Toolbox cognitive measures (Weintraub et al., 2013), two of which were analyzed for this study. The first measure was the PSMT (Dikmen et al., 2014), a brief but well-validated measure of memory ability based on memory for a simple story accompanied by pictures. The PSMT emphasizes spatial, temporal, and narrative relations among constituent elements. PSMT performance was summarized with a normed score not corrected for age (i.e., the "uncorrected scaled score") which had a normative distribution such that mean = 100, SD = 15 (Slotkin et al., 2012).

The second measure was the LSWMT (Tulsky et al., 2014), a brief test of working memory that involves recalling a short list of items sorted and/or ranked on simple criteria (e.g., categorized and ordered by physical size). The LSWMT emphasizes typical attributes of working memory including brief retention and manipulation of information. Scaled scores for the LSWMT had the same properties as the PSMT.

2.2.2 | Analysis of behavioral measures

We analyzed the relationship of task performance with age and sex separately for the two measures (PSMT and LSWMT). We tested the association of task performance with chronological age using Pearson's correlation statistic. Potential differences in task performance due to sex were tested using nonpaired t tests.

2.3 | MRI data collection

2.3.1 | Sites and procedures

MRI data were collected at two sites: data from Omaha-area participants were collected using a Siemens Skyra 3.0 T MRI scanner with a 32-channel head coil; data from Albuquerque-area participants were collected using a Siemens TIM Trio 3.0 T MRI scanner with a 32-channel head coil. Scan site was included as a control regressor for rs-FC analyses (see Section 2.5). For all scanning sessions, participants were instructed to move as little as possible, and comfortable padding was added to fill any extra space inside the head coil.

2.3.2 | Scanning parameters

Structural MRI data were collected with a single, 1-mm isotropic resolution T1-weighted scan sequence using the following parameters: TR = 2,400 ms; TE = 1.94 ms; flip angle = 8°; slice thickness = 1 mm; 192 slices; FOV = 256 mm; base resolution = 256; in-plane acceleration factor (GRAPPA) = 2; acquisition time = 345 s. rs-fMRI data were collected in two T2*-weighted multiband echo-planar imaging (EPI) sequences using the following parameters: TR = 460 ms; TE = 29 ms; flip angle = 44°; slice thickness = 3 mm; 48 slices; FOV = 268 mm; base resolution = 82; multiband acceleration factor = 8; phase encoding direction = anterior–posterior; acquisition time = 306 s; voxel size = 3.3 × 3.3 × 3.0 mm. One resting-state scan was collected with the participant's eyes open, the other with the participant's eyes closed, and order of these conditions was randomly assigned. Single-band EPI reference volumes were collected immediately prior to multiband functional data collection. Two additional datasets were collected for post hoc correction of EPI distortion. These distortion-correction sequences were single-band spin-echo sequences and used the following parameters: TR = 7,220 ms; TE = 73 ms; flip angle = 90°; slice thickness = 3 mm; 48 slices; FOV = 268 mm; base resolution = 82; acquisition time = 22 s; voxel size = 3.3 × 3.3 × 3.0 mm. One distortion correction volume was collected with the same phase-encoding direction as the main EPI volumes (AP) and the other was collected with the phase-encoding direction reversed (PA).

2.4 | MRI data processing

2.4.1 | Structural data

T1-weighted MRI data were converted from DICOM to NIFTI using dcm2niix (Li, Morgan, Ashburner, Smith, & Rorden, 2016), and then rigid-body reoriented to align with a sample-specific template. ANTs software (Avants, Tustison, Wu, Cook, & Gee, 2011; Tustison et al., 2010) was then used for skull-stripping, tissue segmentation, and bias correction. Bias-corrected structural MRI data were also submitted to the FreeSurfer (Fischl, 2004) automated segmentation pipeline (recon-all) for additional parcellation and segmentation. Masks of cerebral white matter and ventricular cerebrospinal fluid were generated from FreeSurfer parcels, eroded to reduce aliasing of adjacent tissue compartments, and used as region-of-interest (ROI) seeds to create regressors which supported processing of functional data (see next section).

The hippocampus was manually segmented using Slicer 3D software. Tracing was carried out in the coronal view, anterior-to-posterior; the anterior-most slice was the first appearance of hippocampus inferior to amygdala; the posterior-most slice was the last appearance of the hippocampus as distinct from the surrounding white matter of the temporal lobe; and tracing respected the anatomical boundaries of the hippocampus (and surrounding MTL tissues) as established by prior work (Duvernoy, 2005; Insausti et al., 1998; Winterburn et al., 2013). All hippocampi were traced by two raters; interrater reliability was >0.8.

Finally, ANTs software was used to generate a nonlinear registration from individual anatomy to the MNI ICBM 152 nonlinear 2009c (henceforth, MNI-152) template space (Fonov, Evans, McKinstry, Almli, & Collins, 2009; Fonov et al., 2011), and the resulting nonlinear warp was retained for use during functional data processing.

2.4.2 | Functional data

T2*-weighted MRI data were converted from DICOM to NIFTI, and then submitted to a processing pipeline using AFNI tools (Cox, 1996) generated with afni_proc.py (Taylor et al., 2018). The first two volumes of each run's EPI data were discarded, leaving 1,296 volumes (i.e., 9.967 min of rs-fMRI data). We combined data from the eyes-open and eyes-closed conditions for our main analysis to enhance the reliability of our rs-FC measures, but we also tested for differences by condition (see Supporting Results). The data were processed as follows: (a) despiking of EPI data; (b) slice-timing correction; (c) nonlinear distortion correction of EPI data based on distortion-correction volumes; (d) alignment of individual T1 anatomy to target EPI volume (single-band EPI volumes were used as a registration target to capitalize on enhanced tissue contrast); (e) applying the nonlinear warp from individual T1 anatomy to MNI-152 template space (see previous section); (f) registration of all EPI volumes to target EPI volume (nb. realignment parameters were retained to be used as control regressors for motion and for calculation of FD); (g) EPI masking to limit data to brain-derived signals; (h) regression with typical confound regressors (mean white-matter signal, mean CSF signal, global signal [conditionally, see below], realignment parameters, and the first derivative of the realignment parameters); (i) band-pass filtering to retain signals between 0.009 and 0.08 Hz (Power, Schlaggar, & Petersen, 2014; Satterthwaite et al., 2013); and (j) spatial smoothing with a 6-mm full-width half-max Gaussian kernel.

During processing, functional volumes with significant evidence of motion (FD > 0.2 mm) and/or a high proportion of signal outliers (>0.1) were flagged for censoring. Regression, band-pass filtering, and later analyses (see below) did not use data at censored timepoints. Band-pass filtering without the use of censored data was implemented by first interpolating values for the censored timepoints based on noncensored timepoints, then applying the band-pass filter, and finally reapplying the original censoring mask to the band-pass-filtered data (Power, Mitra, et al., 2014). All processing was performed twice so that the effects of including/excluding a control regressor representing the global signal (i.e., global signal regression [GSR])

could be evaluated (Murphy & Fox, 2017). Finally, we monitored the number of degrees of freedom retained after preprocessing based on censoring, band-pass filtering, and regression to ensure that sufficient data were retained to support meaningful inference. Using the conservative assumption that all terms were orthogonal and modeled simultaneously, the estimated degrees of freedom consumed during preprocessing operations was 1,227, meaning that a minimum of 1,228 noncensored EPI volumes (9.415 min, 94.8% of total) were necessary for analysis of a dataset.

2.5 | rs-FC analysis

Resting-state T2* data were used to measure the rs-FC of the bilateral hippocampus using a seed-based approach implemented with AFNI's 3dmaskave, 3dTcorr1D, and 3dTtest++ tools. Additionally, the influence of several covariates on the overall pattern of hippocampal rs-FC was evaluated. Participant-related covariates of primary interest were: age; task performance (i.e., PSMT or LSWMT); and the interaction of age with task performance (age × performance). Control covariates were: sex (binary indicator for F/M); scanner site (binary indicator for UNMC or MRN scanner); and median FD for the resting state EPI (estimated from realignment parameters). All analysis of rs-FC was conducted in MNI-152 template space.

The hippocampal seed ROI was empirically generated by warping each participant's manually traced hippocampal mask into EPI space, averaging the binary masks to create a proportional group-mean mask, and thresholding the group-mean mask to create a binary group mask of the hippocampus (bilateral). Anterior and posterior group hippocampal ROI masks were created by dividing the whole-hippocampus ROI mask at the uncal apex. Finally, a control ROI consisting of a binary mask containing atlas gray matter voxels ("all-GM") was created. Analysis of covariance with the all-GM rs-FC was a control measure to ensure that focal covariation with hippocampal rs-FC was not attributable to global effects.

Our rs-FC analysis was conducted as follows: (a) using the ROI masks, mean timeseries for each ROI were calculated for each participant; (b) each mean ROI timeseries was correlated (Pearson's r) with voxelwise timeseries data for the whole brain for each participant to provide whole-brain voxelwise correlation maps; (c) Fisher's Z transform was applied to the voxelwise correlation maps for statistical analysis; (d) statistical tests of voxelwise correlation and covariate values were conducted as voxelwise tests against the null hypothesis (i.e., true value equal to 0) using one-sample, two-sided t tests with linear modeling for covariates (implemented with AFNI's 3dttest++ utility, (Cox, Chen, Glen, Reynolds, & Taylor, 2017)) yielding voxelwise mean values for correlations, β weights for covariates, and associated T values for both; and (e) the resulting statistical maps were thresholded for significance using voxelwise and cluster-extent thresholds (see following paragraphs for details).

Our general approach to evaluating the statistical significance of rs-FC findings used a two-stage process (nb. thresholds for specific analyses are described below): (a) the appropriate statistical map for a given effect was thresholded voxelwise to retain only voxels with statistically significant values and (b) clusterwise thresholding was

applied so that only significant voxels with sufficient adjacency to other significant voxels were retained as clusters. We applied this general approach to overall hippocampal rs-FC and per-effect covariation or difference maps as described next.

For overall hippocampal rs-FC (with and without GSR), much of the brain showed rs-FC that surpassed standard voxelwise/ clusterwise thresholds (Cox et al., 2017; Eklund, Nichols, & Knutsson, 2016; Eklund, Knutsson, & Nichols, 2018). For this reason, we selected stringent thresholds that identified the strongest absolute correlations in the statistical maps to illustrate the spatial distribution of highly significant, spatially extensive clusters of rs-FC (e.g., Blankenship et al., 2017). Specifically, we applied a threshold to select the strongest 5% of absolute voxelwise correlation values in the overall rs-FC maps, and then applied a cluster threshold of 50 voxels. For the overall map of rs-FC without GSR, the threshold for the strongest 5% was $r_Z = .459$, $T(95) = 10.782$, $p < 10^{-17}$; with GSR, the threshold was $r_Z = .260$, $T(95) = 7.394$, $p < 10^{-10}$.

Statistical significance of other rs-FC findings was evaluated using recommended threshold values (Cox et al., 2017; Eklund et al., 2016; Eklund et al., 2018): (a) all statistical maps were thresholded voxelwise to retain only voxels where $p < .001$ ($T(95) = 3.405$) and (b) clusterwise thresholding based on empirically estimated spatial autocorrelation was applied to the thresholded voxelwise maps to enforce a false-discovery rate (FDR) equal to 0.05, here an extent of 24 contiguous (i.e., touching faces) voxels. These clusterwise FDR tests are denoted with "p_c." Spatial autocorrelation in the resting-state EPI data was estimated using AFNI's 3dFWHMx function applied to the nonregressed EPI data of each participant. The parameters of the observed spatial autocorrelation were averaged across all participants, and those group-average spatial autocorrelation parameters were used with AFNI's 3dClustSim function to generate a cluster-extent threshold for the desired FDR (Cox et al., 2017), here 24 voxels. Additionally, for individual clusters meeting the above criteria, we report corrected p values (p_c) based on the cluster's spatial extent to better reflect their statistical significance. We also conducted an exploratory analysis of normative expectations for hippocampal rs-FC based on these analyses (see SI Results).

Spatial similarity of neocortical rs-FC maps for different ROIs (e.g., anterior vs. posterior hippocampus) or different datasets (Dev-CoG vs. Philadelphia Neurodevelopmental Cohort [PNC]) was measured using spatial correlation. Spatial similarity of cluster masks for different processing parameters (e.g., with GSR vs. without GSR) was measured with Dice's coefficient (Dice, 1945). Both measures were calculated using AFNI's 3ddot tool (its -docor and -dodot functions, respectively) and spatially restricted by an EPI-space mask of neocortical gray matter.

We also measured the relationship of within-scan motion to ROI– ROI correlation values (Power, Barnes, Snyder, Schlaggar, & Petersen, 2012). We used a previously reported set of 264 widespread neocortical ROIs (Power et al., 2011) to generate 264 timeseries from each processed dataset, and then generated a 264×264 cross-correlation (i.e., connectivity) matrix to characterize ROI–ROI coactivation. Then, the Fisher's-Z transform of each ROI–ROI pair's connectivity was further correlated with the participant's average estimated FD. Finally, the correlation of ROI–ROI pair's connectivity with participant motion was plotted against ROI–ROI distance to support visual inspection of trends in potentially spurious motion-correlation associations (Power et al., 2012). Please see the Supporting Information for additional details and results.

2.6 | Validation dataset

Findings from the discovery dataset were compared and validated with those from a validation dataset which was drawn from the PNC (Satterthwaite et al., 2016). Data were obtained from the dbGaP platform (dbGaP accession phs000607.v3.p2) and maintained securely under the terms of the data use agreement.

2.6.1 | Participants

Inclusion criteria were matched to Dev-CoG on age (i.e., 9–15 years), availability of behavioral data (see below), and evidence consistent with relatively low motion during MRI. Applying these criteria yielded a sample of $N = 123$.

2.6.2 | MRI data collection

MRI data collection was as described previously for the PNC study (Satterthwaite et al., 2014). Data used for the current study included the T1-weighted structural data and single-band EPI resting-state functional data. Structural MRI data were collected with a single T1-weighted MPRAGE scan sequence using the following parameters: TR = 1,810 ms; TE = 3.5 ms; flip angle = 9°; slice thickness = 1 mm (no gap); 160 slices; FOV = 180/240 mm (RL/AP); matrix = 192/256 (RL/AP); in-plane acceleration factor (GRAPPA) = 2; acquisition time = 208 s. rs-fMRI data were collected in one T2*-weighted single-band gradient-echo EPI (GE-EPI) sequence using the following parameters: TR = 3,000 ms; TE = 32 ms; flip angle = 90°; slice thickness = 3 mm (no gap); 46 slices; FOV = 192 mm; base resolution = 64; phase encoding direction = anterior–posterior; acquisition time = 378 s; voxel size = 3 mm isotropic. Resting-state data were collected with the participant's eyes open and fixated on a crosshair.

2.6.3 | MRI data processing

The same approach was applied to process the dataset as described for the discovery dataset.

2.6.4 | rs-FC analysis

The sample analysis procedures applied to the discovery dataset were applied to the validation dataset. As before, for whole-hippocampus

rs-FC, we applied a threshold to select the strongest 5% of absolute voxelwise correlation values in the overall rs-FC maps, and then applied a cluster threshold of 50 voxels. For the overall map of rs-FC without GSR, the threshold for the strongest 5% was $r_Z = .465$, $T(122) = 9.181$, $p < 2 \times 10^{-15}$; with GSR, the threshold was $r_Z = .236$, $T(122) = 7.994$, $p < 10^{-12}$.

Statistical significance of other rs-FC findings was evaluated using recommended threshold values: (a) voxelwise thresholding where $p < .001$ ($T(122) = 3.374$) and (b) clusterwise thresholding to enforce a FDR equal to 0.05, here an extent of five contiguous (i.e., touching faces) voxels. Spatial autocorrelation and minimum cluster extent threshold were calculated as described for the discovery dataset. We note that the empirical, data-driven procedure used to determine cluster extent thresholds based on observed spatial autocorrelation (Cox et al., 2017) can and should yield different extent thresholds when datasets with different spatial autocorrelations are analyzed. Here, spatial autocorrelation was greater for the discovery dataset than the validation dataset, and this was associated with a larger cluster extent threshold for the discovery dataset than the validation dataset. Although not the focus of the current study, we speculate that this may be attributable to reduced contrast and/or increased noise in the multiband EPI data of the discovery dataset versus the single-band EPI data of the validation dataset.

Finally, for covariates, we tested whether statistically significant clusters observed in the discovery dataset showed similar valence in the validation dataset. Our goal was to evaluate whether local patterns of covariance with hippocampal rs-FC might be evident in the validation dataset, even when a typical whole-brain analysis did not reveal corresponding clusters. Using cluster masks generated through analysis of the covariates in the discovery dataset as a priori ROIs, we tested whether the voxels under the cluster mask showed the same valence (beta weights and T values) in the discovery and validation datasets using single-group T tests.

2.6.5 | Behavioral measures

PNC participants did not complete the NIH Toolbox, but alternative cognitive assessments measuring hippocampal-dependent memory and working memory were available (Moore, Reise, Gur, Hakonarson, & Gur, 2015). Hippocampal-dependent memory ability for PNC participants was instead assessed using the Penn Face Memory Test (PFMT). The PFMT tests recognition of previously studied complex visual stimuli (faces), and performance is supported by (hippocampal-dependent) episodic memory (Moore et al., 2015).

Working memory ability of PNC participants was assessed with the letter N-back (LNB) test. The LNB requires participants to monitor a continuous stream of letter stimuli for a target stimulus that is either constant during a test block (0-back condition) or is updated on each stimulus presentation to be a stimulus seen earlier in the stream (1-back and 2-back). Maintaining, updating, and acting upon recently experienced information are key properties of working memory, and the LNB assesses each of them.

2.7 | Combined analysis

We conducted an exploratory combined analysis of hippocampal rs-FC and covariance with memory and age in the discovery and validation datasets using a meta-analytic approach that incorporated the second-level statistical maps for overall hippocampal rs-FC and covariates (memory and age) from both datasets.

The second-level statistical maps for overall hippocampal rs-FC and covariates (memory and age) produced by the discovery and validation analyses were combined using an established meta-analytic approach well-suited to MRI datasets (Winkler et al., 2016). Specifically, we used Tippet's method to combine p-values voxelwise, while voxelwise correlations and β-weights were mean averaged. Statistical significance for overall hippocampal rs-FC was evaluated with a voxelwise criterion representing the strongest 5% of observed values, here $p < 2 \times 10^{-14}$, and a cluster extent threshold of 50 voxels. Statistical significance of covariance with rs-FC findings was also evaluated with voxelwise and cluster extent thresholds: (a) voxelwise thresholding where the combined $p < .001$, one-sided and (b) clusterwise thresholding to enforce an FDR of 0.01, here an extent of 20 contiguous (i.e., touching faces) voxels. Spatial autocorrelation and minimum cluster extent threshold were calculated as described for the independent datasets but used the mean spatial autocorrelation parameters from the discovery and validation datasets as consensus values.

3 | RESULTS

The results of the primary, discovery dataset are presented first, followed by findings from the validation dataset (including comparisons between the two datasets).

4 | DISCOVERY DATASET (DEV-COG)

4.1 | rs-FC of the whole hippocampus

We observed a pattern of rs-FC (controlled for age) for the whole (bilateral) hippocampus (Figure 2) resembling that of prior reports which described young adults (Kahn et al., 2008; Vincent et al., 2006) and children (Blankenship et al., 2017). In particular, we observed strong positive correlations between hippocampus and regions including parahippocampal gyrus, temporal pole, anterior lateral temporal lobe, posterior cingulate/precuneus, ventromedial prefrontal cortex, and posterior inferior parietal lobule/angular gyrus. Findings with-GSR analysis are described below; findings without GSR are provided in the Supporting Information (SI) along with tests of GSR-dependent effects.

Whole-hippocampus rs-FC (with GSR) showed strong positive correlations with regions including parahippocampal gyrus, temporal pole, anterior lateral temporal lobe, posterior cingulate/precuneus, ventromedial prefrontal cortex, and left posterior inferior parietal
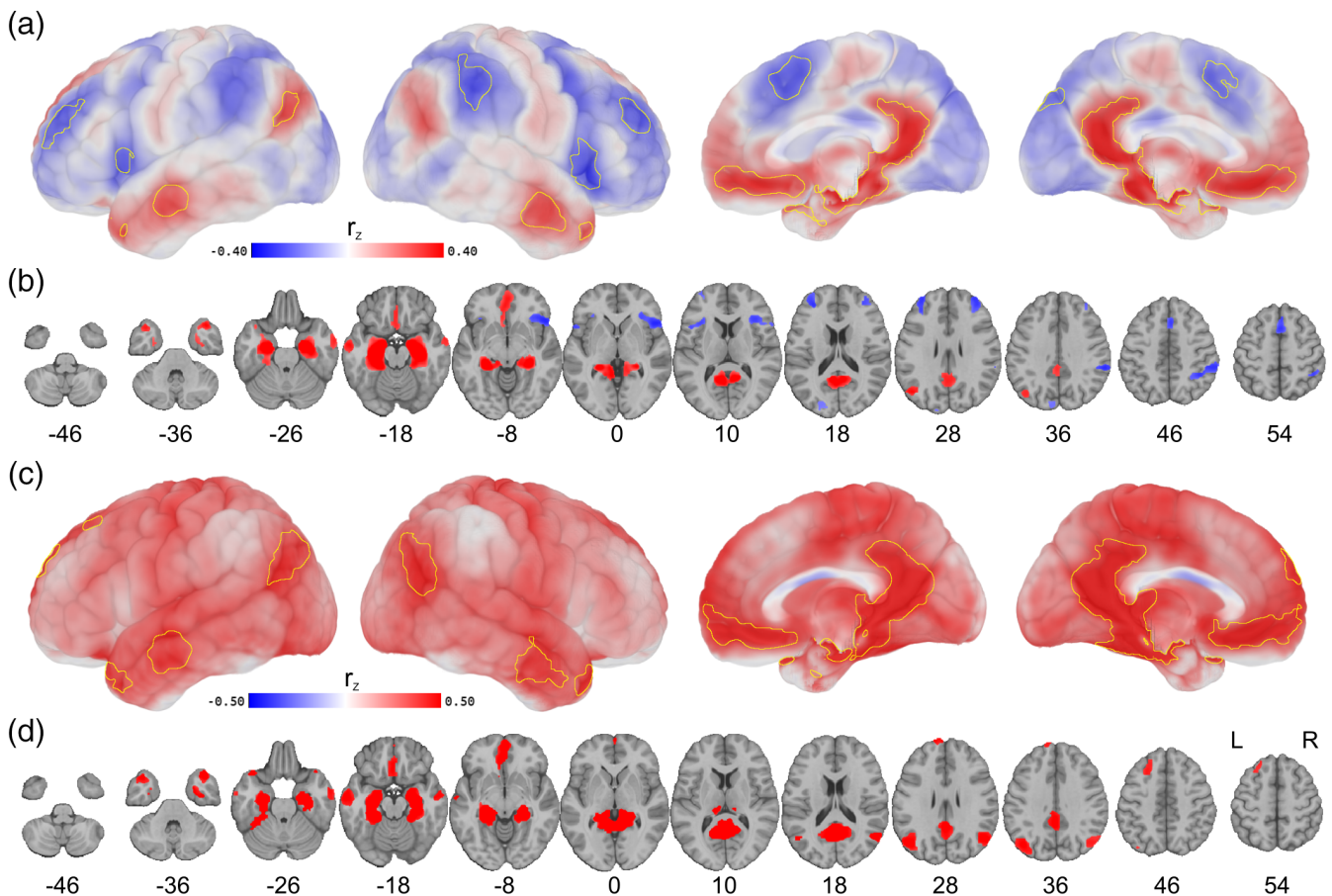
FIGURE 2 Overall hippocampal resting-state functional connectivity (rs-FC) in the discovery dataset with global signal regression (GSR) (a,b) and without GSR (c,d) depicted on the MNI-152 template brain. Yellow outlines highlight clusters of the strongest 5% absolute rs-FC values (voxelwise threshold, max. $p < 10^{-10}$; min. cluster extent of 50 voxels, $p_c < 10^{-10}$; see also Tables 1 and SI 1). (a,c) Three-dimensional renderings showing spatial patterns of hippocampal rs-FC (perspectives, left to right: left lateral, right lateral, right medial, left medial). As expected, negative correlations (blue) are principally evident in the results of the analysis with GSR (a). (b,d) Axial slices showing the same clusters of strong correlation values superimposed on template anatomy. Slices are presented in neurological orientation, and numbers below slices are MNI-152 Z-coordinate values

lobule/angular gyrus (Figure 2a,b, Table 1). Regression of global signal also had the expected consequence of revealing some negative rs-FC values (Murphy & Fox, 2017), and this yielded negative rs-FC clusters in bilateral frontal operculum, bilateral middle frontal gyrus, bilateral superior frontal gyrus, right inferior parietal lobule, left superior parietal lobule, and left fusiform gyrus.

4.1.1 | Covariance with age

Age significantly covaried with whole-hippocampal rs-FC (with GSR) in a region-specific fashion (Figure 3a,d, Table 2). Specifically, right inferior parietal lobule showed significant positive covariance with age ($p_c < .005$) while deep left supramarginal gyrus/insula showed significant negative covariance with age ($p_c < .05$). A cluster in right cerebellar cortex also showed significant positive covariance with age ($p_c < .05$). Regarding the directionality of these findings, positive covariance with age indicated greater hippocampal rs-FC in older children (or less hippocampal rs-FC in younger children) in R IPL and right

cerebellar cortex, while negative covariance with age indicated less hippocampal rs-FC in older children (or greater hippocampal rs-FC in younger children) in L SMG/insula. Further, the L SMG/insula cluster was in the vicinity of a previously reported left superior temporal gyrus cluster that showed an age-related increase in hippocampal rs-FC in younger children (X = −64, Y = −20, Z = +9) (Blankenship et al., 2017). Importantly, none of these significant clusters of hippocampal rs-FC covariance with age overlapped the single gray matter cluster of all-GM rs-FC covariance with age (right superior frontal gyrus; peak X = 10, Y = 1, Z = 76; extent 46 voxels), suggesting that the observed, focal covariance was not attributable to global effects. Findings without GSR are described in the SI.
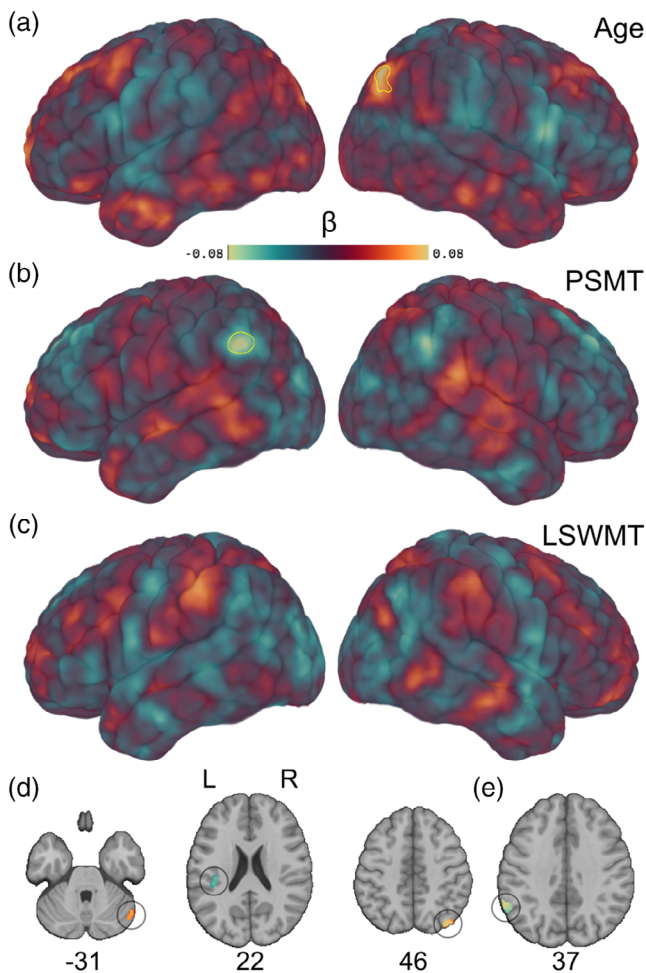
4.1.2 | Covariance with memory ability

Scores on the PSMT negatively covaried with hippocampal rs-FC (with GSR) in one cluster in left supramarginal gyrus, $p_c < .01$ (Figure 3b, Table 2). In this region, greater PSMT scores were

#	k	T	v	x	y	z	Region(s)
1	2,114	27.646	+	−26	−20	−16	Bilateral hippocampus
							Bilateral precuneus
							Bilateral parahippocampal gyrus
							Bilateral amygdala
							Bilateral fusiform gyrus
							Bilateral cingulate gyrus (isthmus)
							Bilateral thalamus proper
							Bilateral ventral midbrain
							Bilateral superior temporal gyrus
							Bilateral entorhinal cortex
							Bilateral middle temporal gyrus
							Bilateral cerebellar cortex
							Bilateral temporal pole
							Bilateral posterior cingulate
2	275	11.891	+	−2	44	−10	Bilateral medial orbitofrontal cortex
							Bilateral rostral anterior cingulate gyrus
							Left nucleus accumbens
3	270	11.557	−	52	20	−4	Right pars opercularis
							Right pars triangularis
							Right insula
							Right lateral orbitofrontal cortex
							Right precentral gyrus
							Right superior temporal gyrus
							Right pars orbitalis
4	196	10.16	−	58	−38	40	Right supramarginal gyrus
							Right superior parietal lobule
							Right inferior parietal lobule
5	131	10.075	−	−34	46	20	Left middle frontal gyrus (rostral)
6	121	9.924	−	38	46	26	Right middle frontal gyrus (rostral)
7	117	10.332	−	2	14	56	Bilateral superior frontal gyrus
							Right caudal anterior cingulate
8	89	9.277	−	−40	16	8	Left pars opercularis
							Left precentral gyrus
							Left lateral orbitofrontal cortex
							Left insula
							Left pars triangularis
9	88	10.338	−	−8	−86	40	Left superior parietal lobule
							Left lateral occipital gyrus
							Left cuneus
10	80	9.687	+	64	−2	−26	Right middle temporal gyrus
11	77	9.56	+	−50	−68	26	Left inferior parietal lobule
12	64	10.418	+	−62	−10	−16	Left middle temporal gyrus

Note: #, ordinal rank of cluster by volume; k, cluster volume (voxels); T, T-statistic value; v, valence (positive or negative); *xyz*, coordinate of cluster's peak RSFC in MNI-152 template space (LPI).
Abbreviations: GSR, global signal regression; LSWMT, List Sorting Working Memory Test; rs-FC, resting-state functional connectivity.

TABLE 1 Coordinates of peak correlation value (Fisher's Z-transformed Pearson's *r*) in clusters having significant rs-FC with bilateral hippocampus with GSR

FIGURE 3 Age and memory ability showed regional covariance with whole-hippocampus resting-state functional connectivity (rs-FC) with global signal regression (GSR) in the discovery dataset (see also Table 2). (a,d) Chronological age covaried significantly with hippocampal rs-FC in right inferior parietal lobule and deep left supramarginal gyrus/insula. (b,e) Performance on the Picture-Sequence Memory Test (PSMT) covaried significantly with hippocampal rs-FC in left posterior supramarginal gyrus. (c) There were no significant clusters of covariance between performance on the List Sorting Working Memory Test (LSWMT) and hippocampal rs-FC, and the overall spatial pattern of covariance was substantially different than that of age or PSMT performance (a vs. c). For all panels, red-orange colors indicate greater positive covariance with hippocampal rs-FC; blue-green colors indicate negative covariance with hippocampal rs-FC. Yellow lines highlight clusters of voxels which differed significantly (voxelwise threshold, $p < .001$; cluster extent threshold, $p_c < .05$)

associated with lower hippocampal rs-FC. Notably, no significant clusters of covariance with PSMT were evident in the covariance of PSMT scores and rs-FC of the all-GM control ROI, suggesting that this covariance was not attributable to global effects. Meanwhile, scores on the LSWMT did not covary significantly with hippocampal rs-FC in any brain region (Figure 3c). Spatial correlation between covariance maps of PSMT and LSWMT indicated some spatial similarity

(Pearson's $r = .330$, $p < .001$), but visual inspection also indicated substantial differences (Figure 3b,c). Findings without GSR are described in the SI.

4.2 | rs-FC of the anterior and posterior hippocampus

Anterior and posterior portions of the hippocampus showed largely overlapping spatial patterns of rs-FC (with GSR) (Figure 4a–d), but some differences in regional rs-FC strength were evident (Figure 4e,f). Regarding the similarity of posterior and anterior hippocampal rs-FC, the two rs-FC maps exhibited a robust positive spatial correlation with each other ($r = .880$, $p < .001$) and with whole-hippocampus rs-FC (anterior-whole $r = .983$; posterior-whole $r = .952$; each $p < .001$). Consistent with these spatial correlations, anterior and posterior hippocampus were associated with significant clusters of rs-FC distributed across similar regions as each other and the whole hippocampus.

However, there was a set of regions (largely midline) that showed significant differences in rs-FC strength for anterior and posterior hippocampus (Table 3). Anterior hippocampus was found to have stronger rs-FC in dorsal precentral gyrus/paracentral lobule, right inferior temporal gyrus/fusiform gyrus, and (as expected) anterior hippocampus. Posterior hippocampus was found to have stronger rs-FC in bilateral precuneus, bilateral posterior cingulate, right anterior cingulate, and (as expected) posterior hippocampus. These patterns were generally consistent with prior reports on the differences between anterior and posterior hippocampal rs-FC in midline regions for younger children (Blankenship et al., 2017).

There were no statistically significant clusters of covariance between anterior–posterior hippocampal rs-FC and age, memory ability, or their interaction term. Findings without GSR are described in the SI.

4.3 | Behavior

We tested behavioral measures (PSMT, LSWMT, and median FD during resting-state data collection) for correlations with chronological age and for differences by sex. We did not observe any statistically significant correlations or differences. However, there was a significant, positive correlation between scores on the PSMT and LSWMT.

4.3.1 | Picture-Sequence Memory Test

Scores on the PSMT (not corrected for age, see Section 2) were consistent with normative expectations and showed evidence of individual variability (mean = 112.5, SD = 11.2). There was not a significant correlation between PSMT scores and age ($T(94) = 0.723$, $p = .472$, Pearson's $r = .074$), and scores did not differ by sex ($T(94) = 0.154$, $p = .878$).

TABLE 2 Coordinates of peak covariance (β weight) in clusters having significant covariance between bilateral whole hippocampal rs-FC (with GSR) and participant-level covariates (memory [PSMT score], age, and interaction term). No statistically significant clusters were observed for covariance with LSWMT scores

Covariate	#	k	T	v	x	y	z	Region(s)
Memory	—	35	4.272	—	−62	−50	38	Left supramarginal gyrus
								Left inferior parietal lobule
Age	1	43	4.210	+	40	−76	50	Right superior/inferior parietal lobule
	2	27	4.366	+	50	−70	−32	Right cerebellar cortex
	3	27	4.634	—	−38	−26	22	Left insula
Age × Memory	—	27	4.764	+	44	−52	−34	Right cerebellar cortex

Note: #, ordinal rank of cluster by volume; *k*, cluster volume (voxels); *T*, *T*-statistic value; *v*, valence (positive or negative); *xyz*, coordinate of cluster's peak RSFC in MNI-152 template space (LPI).

Abbreviations: GSR, global signal regression; LSWMT, List Sorting Working Memory Test; PSMT, Picture-Sequence Memory Test; rs-FC, resting-state functional connectivity.

4.3.2 | List Sorting Working Memory Test

Scores on the LSWMT (not corrected for age, see Section 2) were consistent with normative expectations and showed evidence of individual variability (mean = 105.0, SD = 10.9). There was not a significant correlation between LSWMT scores and age ($T(94) = 1.719$, $p = .089$, Pearson's $r = .175$), and scores did not differ by sex ($T(94) = 0.808$, $p = .421$).

4.3.3 | PSMT and LSWMT

Scores on the PSMT and LSWMT were significantly positively correlated ($T(94) = 3.910$, $p < .001$, Pearson's $r = .374$). The approximately 14% shared variance between the two measures likely reflected some reliance on shared cognitive processes, but the remaining 86% nonshared variance indicated substantial contributions from task-unique cognitive abilities (as well as individual differences, noise in measurement, etc.).

4.3.4 | Framewise displacement

Median FD was moderate and showed limited variability (mean = 0.112 mm, SD = 0.020 mm). There was not a significant correlation between median FD and age ($T(94) = 0.975$, $p = .332$, Pearson's $r = −.100$) although the negative valence of the (nonsignificant) correlation was in the expected direction (i.e., older children exhibited numerically less motion). Median FD did not differ by sex ($T(94) = 1.031$, $p = .305$).

5 | VALIDATION DATASET (PNC)

5.1 | Overview

Observations from the validation dataset (PNC) were broadly consistent with those from the discovery dataset (Dev-CoG). This included the patterns of whole-hippocampus rs-FC (Figure 5), as well as evidence for focal covariance of hippocampal rs-FC with memory ability in lateral parietal regions and similar spatial covariance of hippocampal rs-FC with age (Figure 6). Focused highlights of the validation analysis with GSR are described below; rs-FC cluster tables without GSR are presented in the SI.

5.2 | rs-FC of the whole hippocampus

Whole-hippocampus rs-FC was highly similar between the discovery and validation datasets (Figure 5). The spatial correlation of rs-FC maps was positive, robust, and statistically significant (Pearson's $r = .895$, $p < .001$). Consistent with this, clusters of statistically significant whole-hippocampus rs-FC were highly overlapping (Dice's coefficient = 0.535).

5.2.1 | Covariance with age

Covariance of whole-hippocampus rs-FC with age was similar between the discovery and validation datasets (Figure 6). The spatial correlation of rs-FC covariance maps was strong, positive, and statistically significant (Pearson's $r = .377$, $p < .001$). Despite this overall similarity, focal clusters of statistically significant covariance did not overlap between the two datasets.

5.2.2 | Covariance with memory ability

Covariance of whole-hippocampus rs-FC with hippocampal-dependent memory ability (Dev-CoG, PSMT; PNC, PFMT) showed similar concentrations in lateral parietal cortex in the discovery and validation datasets (Figure 6). The spatial correlation of rs-FC covariance maps was numerically moderate but statistically significant (Pearson's $r = .175$, $p < .001$). Critically, a left-lateralized IPL cluster of rs-FC covariance from the discovery dataset was mirrored in a right-lateralized IPL cluster in the validation dataset. Ignoring laterality, the
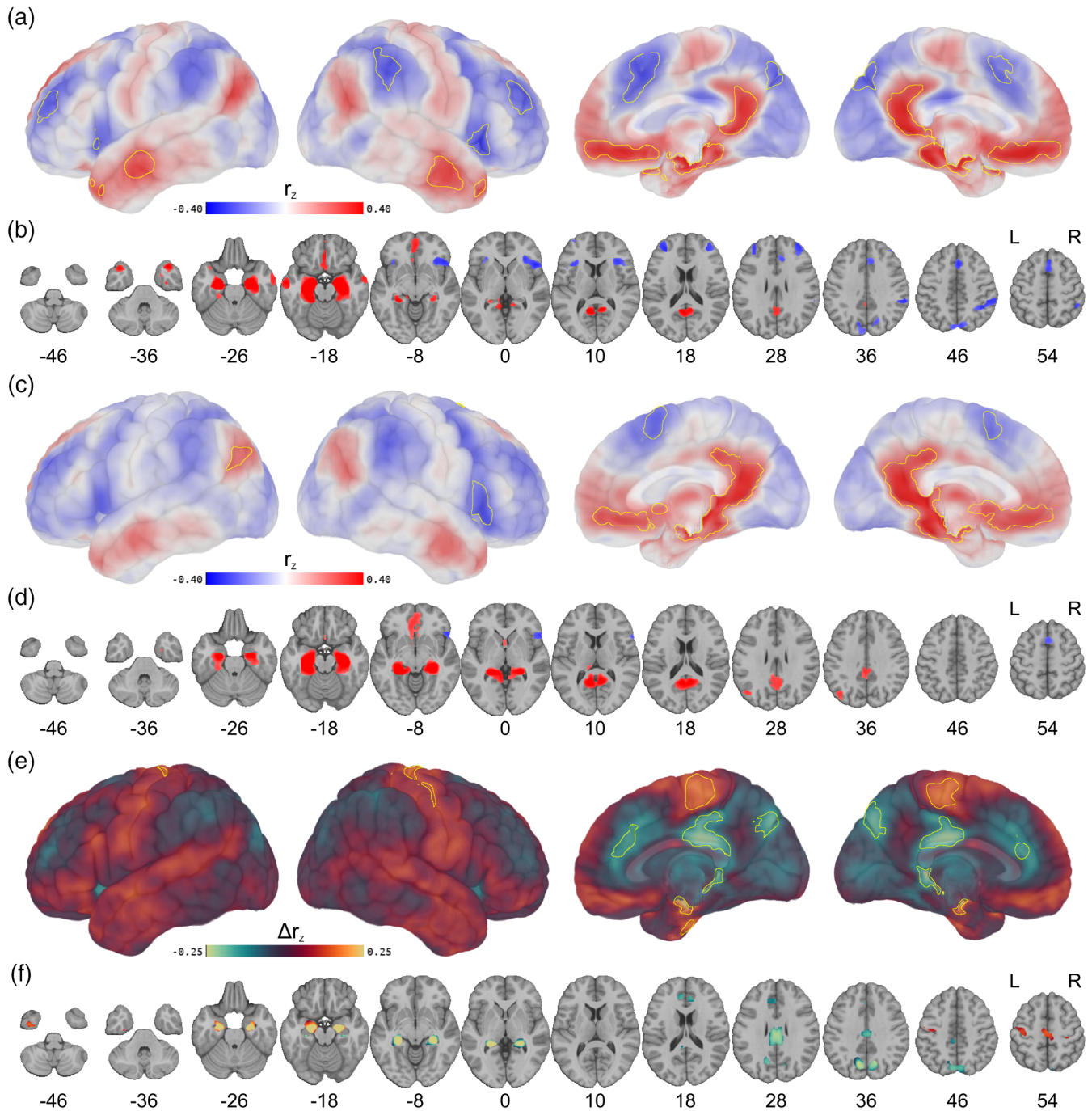
FIGURE 4 Anterior and posterior hippocampus showed moderate differences in the spatial patterns of resting-state functional connectivity (rs-FC) in the discovery dataset. Anterior hippocampus exhibited greater rs-FC in paracentral lobule and near the central sulcus; posterior hippocampus exhibited greater rs-FC in anterior cingulate, posterior cingulate, and precuneus (see also Table 3). Yellow outlines highlight clusters of the strongest rs-FC values (voxelwise threshold, max. $p < 10^{-10}$; min. cluster extent of 50 voxels, $p_c < 10^{-10}$; see also Tables 1 and SI 1). (a,c) Three-dimensional renderings showing spatial patterns of anterior (a) and posterior (c) hippocampal rs-FC (perspectives, left to right: left lateral, right lateral, right medial, left medial). (b,d) Axial slices showing the same clusters of strong correlation values superimposed on template anatomy for anterior (b) and posterior (d) hippocampus. (e,f) Differences between anterior and posterior hippocampal rs-FC are shown using the same three-dimensional perspectives and axial slices as (a–d). Red-orange colors indicate greater anterior hippocampal rs-FC; blue-green colors indicate greater posterior rs-FC. Yellow lines highlight clusters of voxels which differed significantly (voxelwise threshold, $p < .001$; cluster threshold, $p_c < .05$). Regions showing statistically greater rs-FC with posterior hippocampus were more spatially extensive (anterior and posterior cingulate, precuneus, retrosplenial cortex) than those of anterior hippocampus (paracentral lobule, primary somatosensory regions)

#	k	T	v	x	y	z	Region(s)
1	589	5.074	+	14	−16	70	Bilateral precentral gyrus
							Bilateral paracentral lobule
							Bilateral postcentral gyrus
2	257	4.93	−	16	−68	34	Bilateral precuneus
							Bilateral superior parietal lobule
							Right cuneus
3	232	5.458	−	−2	−20	28	Bilateral posterior cingulate
							Right paracentral lobule
							Right cingulate gyrus (isthmus)
							Right precuneus
4	173	9.111	−	−22	−38	−2	Left hippocampus
							Left thalamus proper
							Left ventral midbrain
5	134	10.038	+	20	−10	−20	Right hippocampus
							Right amygdala
							Right ventral midbrain
6	127	8.493	−	28	−28	−10	Right hippocampus
							Right thalamus proper
							Right ventral midbrain
7	103	9.049	+	−22	−14	−20	Left hippocampus
							Left amygdala
							Left ventral midbrain
8	64	4.108	−	8	38	20	Right caudal anterior cingulate
							Right rostral anterior cingulate gyrus
9	44	4.549	+	40	−8	−46	Right inferior temporal gyrus
							Right fusiform gyrus

TABLE 3 Coordinates of peak difference in correlation value (Fisher's Z-transformed Pearson's r) in clusters having significant rs-FC with anterior vs. posterior hippocampus with GSR. Positive valence (+) indicates stronger rs-FC with anterior hippocampus; negative valence indicates stronger rs-FC with posterior hippocampus

Note: #, ordinal rank of cluster by volume; k, cluster volume (voxels); T, T-statistic value; v, valence (positive or negative); xyz, coordinate of cluster's peak RSFC in MNI-152 template space (LPI).
Abbreviations: GSR, global signal regression; rs-FC, resting-state functional connectivity.

two supramarginal-gyrus clusters showed strict adjacency (i.e., faces-touching voxels).

Further, we observed a regional pattern of beta weights and statistic values that was consistent with reliable negative covariance between hippocampal rs-FC and memory performance in the same left supramarginal gyrus cluster as the discovery dataset (which showed negative covariance between memory and hippocampal rs-FC). Regarding valence, 34 of 35 voxelwise ROI beta weights in the validation covariance map were negative, the mean beta weight in the cluster was $\beta = -.033$, and the beta weights were significantly less than zero ($T(34) = -12.878$, $p < .001$). Regarding statistical significance, the mean voxelwise T value was $T(119) = -1.691$, $p = .047$. These results are consistent with negative covariance in this left SMG ROI between memory (here, PFMT) and hippocampal rs-FC in the validation dataset. Thus, while the association was less statistically robust in the validation dataset, a pattern of focal (left SMG) negative covariance between hippocampal rs-FC and memory performance was consistent across the discovery and validation datasets.

Covariance of whole-hippocampus rs-FC with working memory ability (Dev-CoG, LSWMT; PNC, LNB) showed similar spatial distributions in the discovery and validation datasets (Figure 6). The spatial correlation of rs-FC covariance maps was numerically moderate but statistically significant (Pearson's $r = .181$, $p < .001$). There were no focal clusters of statistically significant covariance for working memory ability in the discovery dataset, thus precluding analysis of cluster overlap.

5.2.3 | Covariance, spatial similarity between datasets

As described above, there was evidence of spatial similarity (statistically significant positive correlations) between the covariance of whole-hippocampus rs-FC with age, hippocampal-dependent memory, and working memory across the discovery and validation datasets. Additionally, a full cross-correlation of these covariate statistical maps
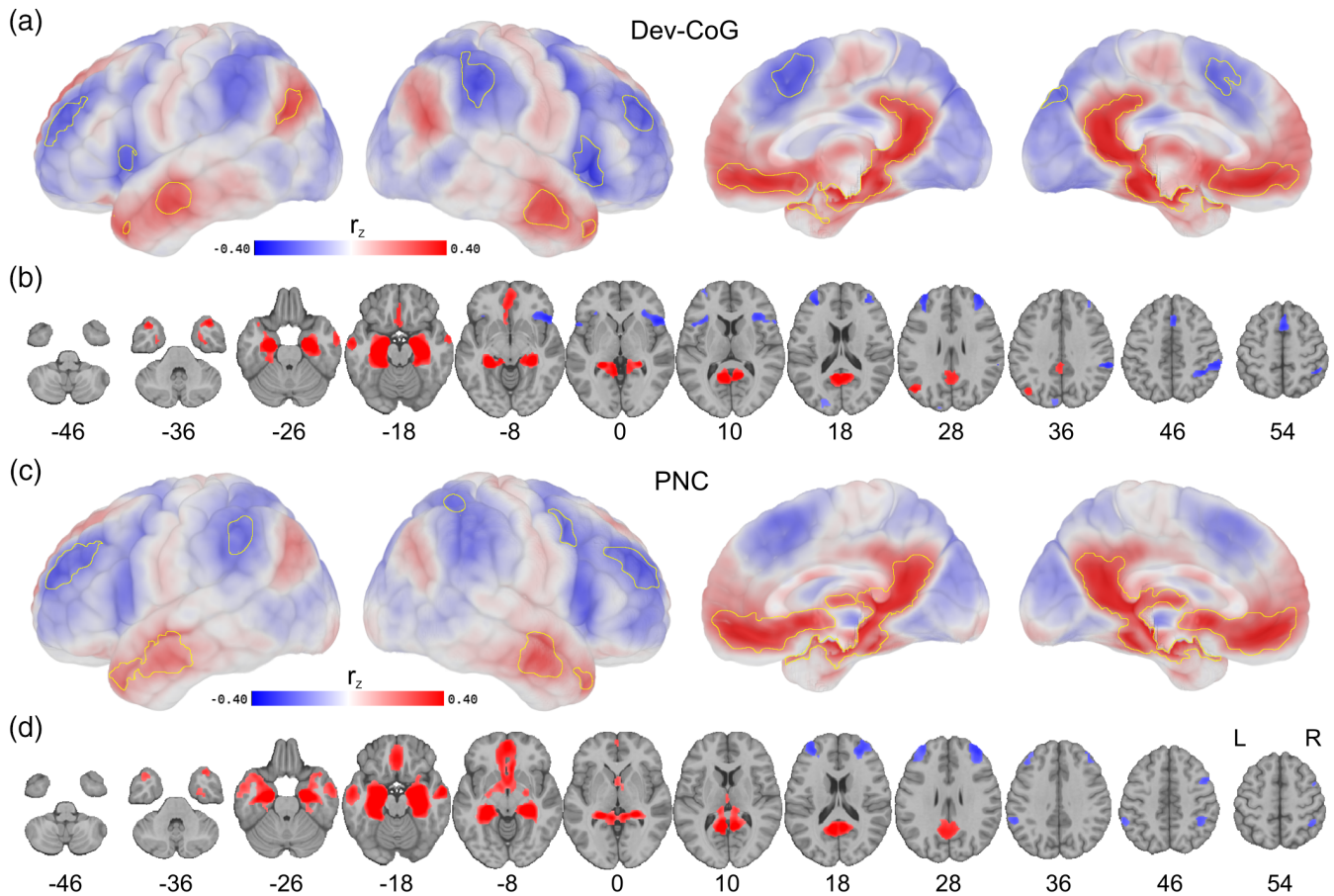
FIGURE 5 Comparison of overall hippocampal resting-state functional connectivity (rs-FC) in the discovery dataset (Developmental Chronnecto-Genomics [Dev-CoG], a,b) and the validation dataset (Philadelphia Neurodevelopmental Cohort [PNC], c,d) with GSR. The similarity of overall hippocampal rs-FC in the two datasets was readily apparent and statistically robust. See Figure 2 caption for additional information; note that Dev-CoG findings from Figure 2a,b are reproduced here for reference

across datasets ($3 \times 3 = 9$ total correlations) showed that these were the three largest correlation values. That is, spatial correlation of covariance maps from the Dev-CoG and PNC datasets was greatest when the Dev-CoG age covariance map was compared to the PNC age covariance map (rather than when age was compared to working memory, for example). The probability that the three matching pairs of covariates across datasets would be associated with the three strongest correlations by chance was $1 \div \binom{9}{3} = 1.19\%$. Our observation of this low probability outcome is consistent with our findings that the measures and their covariance with whole-hippocampus rs-FC were much more similar between datasets than would be expected by chance.

5.3 | rs-FC of the anterior and posterior hippocampus

Anterior and posterior portions of the hippocampus showed rs-FC that was highly similar between the discovery and validation datasets. Spatial correlation between the discovery and validation datasets was high for both, with Pearson's $r = .894$, $p < .001$ and Pearson's $r = .888$, $p < .001$

for the anterior and posterior hippocampal seed regions, respectively. Clusters of statistically significant anterior-hippocampus rs-FC were highly overlapping (Dice's coefficient = 0.502), as were those of the posterior hippocampus (Dice's coefficient = 0.626).

6 | COMBINED DATASET (DEV-COG AND PNC)

An exploratory analysis which combined second-level statistical maps from the discovery and validation datasets using a meta-analytic approach produced results that were generally consistent with one or both earlier analyses.

6.1 | rs-FC of the whole hippocampus

Hippocampal rs-FC in the combined dataset strongly resembled the findings from the individual datasets (Figure 7a). Given the high spatial correlation observed between the discovery and validation datasets, this was consistent with expectations.
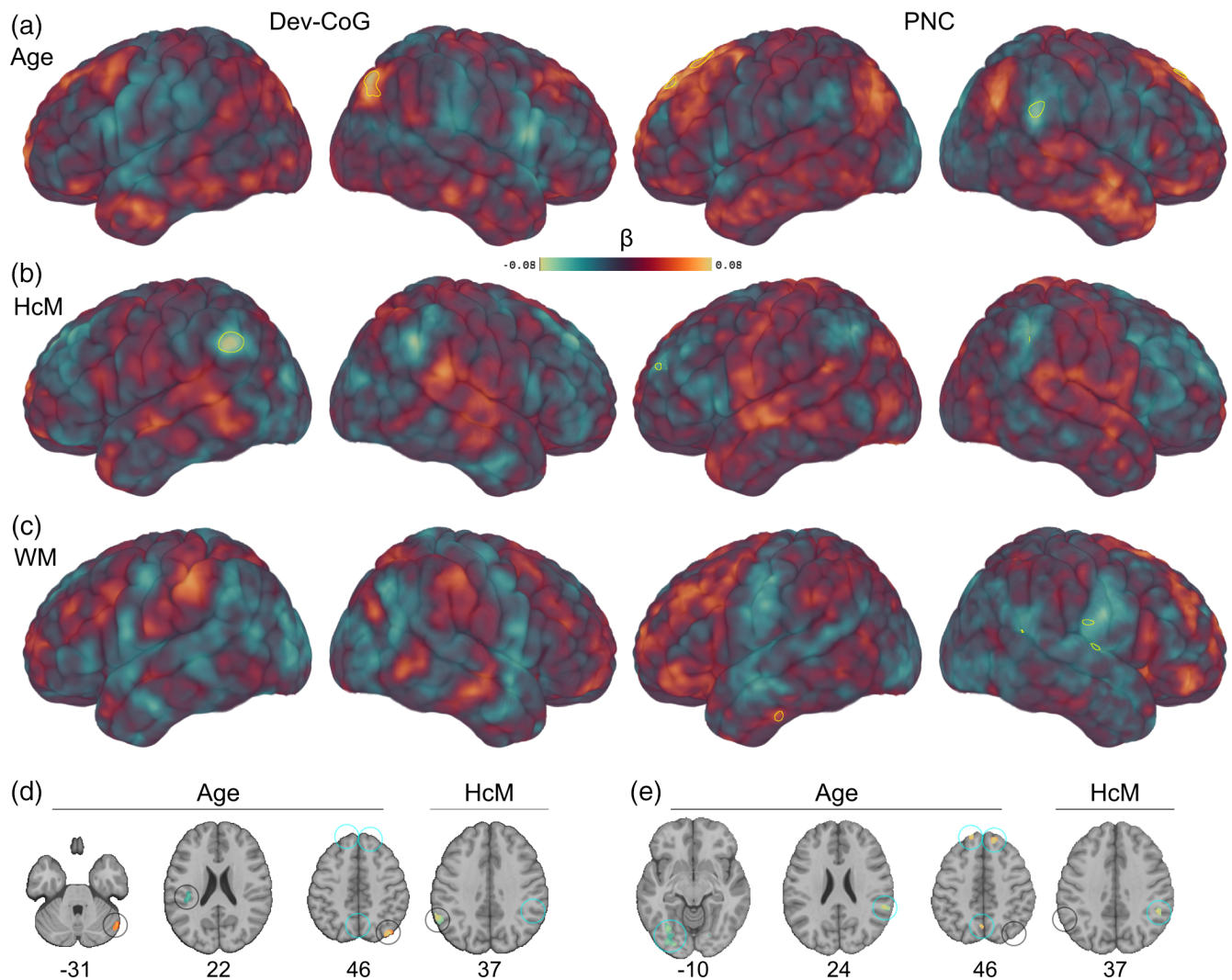
FIGURE 6 Comparison of hippocampal resting-state functional connectivity (rs-FC) covariance with age and memory ability in the discovery dataset (Developmental Chronnecto-Genomics [Dev-CoG], left two columns) and the validation dataset (Philadelphia Neurodevelopmental Cohort [PNC], right two columns). Among the covariates, age (Panels a,d,e) exhibited the greatest spatial correlation between the two datasets (Pearson's $r = .377$, $p < .001$). Hippocampal-dependent memory (HcM; Panels b,d,e) also demonstrated a significant spatial correlation (Pearson's $r = .175$, $p < .001$), and across datasets there were significant clusters in highly similar regions of IPL/supramarginal gyrus (Dev-CoG, left-lateralized; PNC, right-lateralized). Working memory (WM; Panel c) also produced spatially similar covariance maps (Pearson's $r = .181$, $p < .001$), but there were no statistically significant clusters for the discovery dataset. In Panels (d) and (e), statistically significant clusters are circled for the discovery (dark) and validation (light) datasets. Further, on axial slices common to Panels (d) and (e) ($Z = +37$ and $Z = +46$), these cluster-highlighting circles (but not the corresponding clusters) are shown for the same covariate from the alternate dataset to facilitate comparison of cluster locations across datasets. See Figure 3 caption for additional information; note that the discovery dataset findings from Figure 3 are reproduced here for reference. HcM, hippocampal-dependent memory ability; WM, working memory ability

6.2 | Covariance with memory ability

The combined analysis of hippocampal rs-FC with hippocampal-dependent memory identified a single cluster in left IPL/SMG ($p_c < .05$) in the locale of the memory-covariance cluster in the discovery dataset (Figure 7b and SI Table 4). Tests for covariance with working memory did not identify any statistically significant clusters.

6.3 | Covariance with age

The combined analysis of hippocampal rs-FC with age identified several clusters (each $p_c < .05$), all of which were in the locale of clusters

identified in the memory-covariance analysis of the validation dataset (Figure 7c and SI Table 4).

7 | DISCUSSION

In our study of hippocampal rs-FC in healthy periadolescent children, we found that the hippocampus exhibited functional connectivity with a widespread network of brain regions including portions of prefrontal, temporal, parietal, and cingulate cortex. This intrinsic hippocampal network has not been previously described in periadolescent children, so our findings represent a novel, logical midpoint between descriptions of the same network from samples of younger children
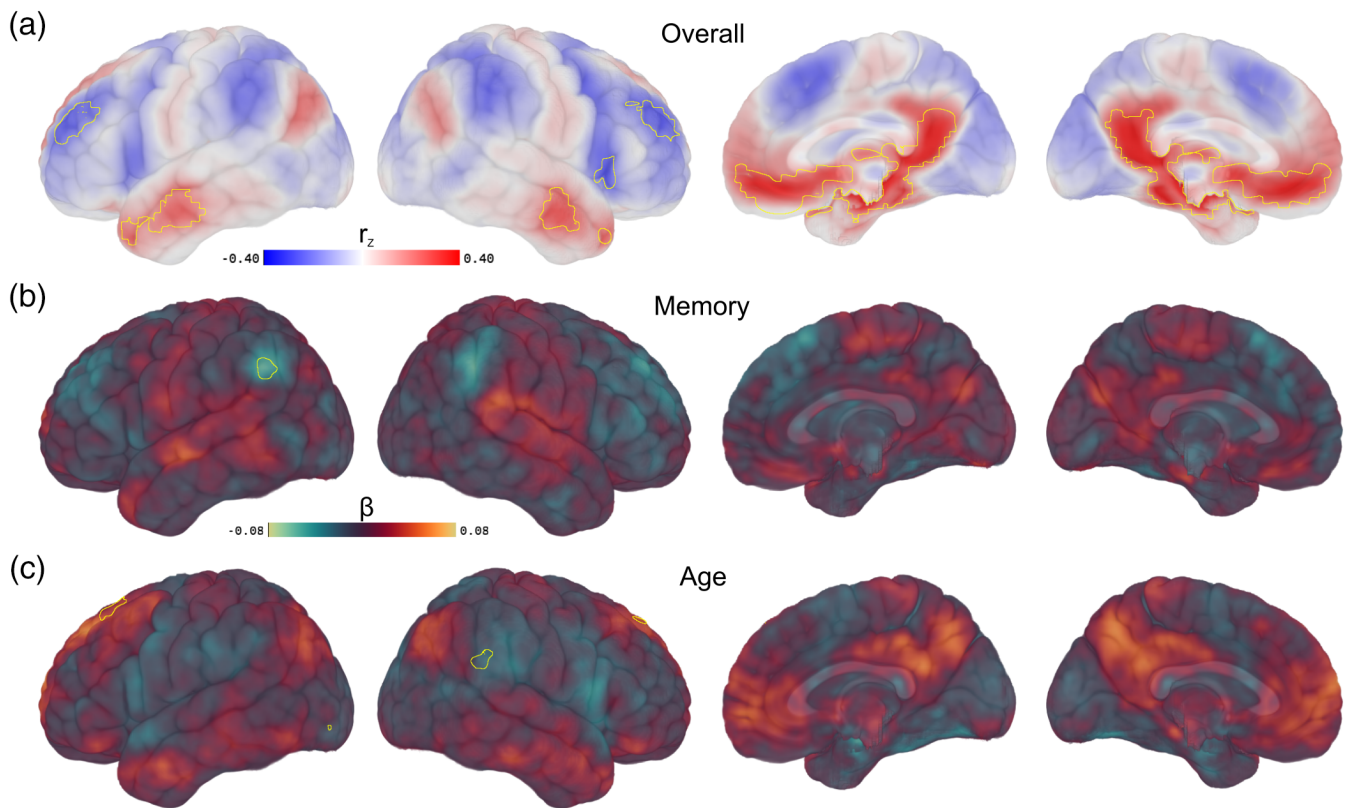
FIGURE 7 Combined analysis of hippocampal resting-state functional connectivity (rs-FC) and covariance across the discovery (Developmental Chronnecto-Genomics [Dev-CoG]) and validation (Philadelphia Neurodevelopmental Cohort [PNC]) datasets. (a) Overall hippocampal rs-FC in the combined dataset reflected the same general patterns observed in the discovery dataset and conserved in the validation dataset. (b) The combined analysis of covariance of hippocampal-dependent memory performance with hippocampal rs-FC identified a single negative-valence cluster in left IPL/left SMG. This cluster was in the locale of the memory-covariance cluster identified in the discovery dataset. No significant clusters were identified in the analysis of covariance with working memory. (c) The combined analysis of covariance of age with hippocampal rs-FC identified several clusters of significant covariance in the locale of clusters identified in the validation dataset

(principally ages 4–8 years) (Blankenship et al., 2017; Geng et al., 2019) and young adults (ages 18–34 years) (Kahn et al., 2008; Vincent et al., 2006). Further, we found that age and memory significantly modulated the overall pattern of hippocampal rs-FC in that these variables were associated with unique, focal changes in rs-FC patterns, and that this focal covariance was not driven by global effects. Importantly, many brain-wide and regional elements of hippocampal rs-FC were observed in both the discovery and validation datasets, and a combined analysis using a meta-analytic approach also found evidence of regionally specific covariation. These findings suggest that many of our observations are robust and could reasonably be expected to generalize beyond the current study. Our findings align with prior work on hippocampal rs-FC in younger and older individuals while filling a key gap in the literature by characterizing this network in periadolescent children.

7.1 | Toward a full characterization of hippocampal rs-FC in development

Our findings bridge the putative developmental continuity in hippocampal rs-FC implied (but not previously demonstrated) by studies of early/middle childhood and young adulthood (Blankenship et al., 2017; Kahn et al., 2008; Riggins et al., 2016; Vincent et al., 2006).

The intrinsic functional network associated with bilateral whole hippocampus was similar in extent to previous reports from younger children (Blankenship et al., 2017) and young adults (Kahn et al., 2008; Vincent et al., 2006). One difference between our study of periadolescent children and previous work with young adults (Kahn et al., 2008; Vincent et al., 2006) was with our finding of rs-FC between the hippocampus and bilateral middle temporal gyrus—Kahn et al. (2008) found that lateral temporal regions showed preferential rs-FC with perirhinal/entorhinal cortex rather than hippocampus. Interestingly, Blankenship et al. (2017) found hippocampal rs-FC with lateral temporal regions that was consistent with our observations.

Potential explanations for regional variability of hippocampal rs-FC between age groups could be theoretically intriguing. For example, there may be an age-related trajectory for connectivity with lateral temporal regions such that hippocampal connectivity during childhood is attenuated by adulthood. Alternatively, the differences could reflect outcome variation due to study-specific methodological decisions regarding MRI data collection, preprocessing, rs-FC seed selection, thresholding, or analysis techniques (Ciric et al., 2017; Poldrack

et al., 2017). Future investigations could provide insight regarding lateral temporal rs-FC with the hippocampus, as well as other issues in the development of hippocampal rs-FC, by applying identical methodological approaches to cross-sectional data sampling children, adolescents, and adults as has been conducted for DMN (Chai et al., 2014a).

7.2 | Memory and hippocampal rs-FC

We observed focal, selective, and negative covariation between declarative/relational memory ability and intrinsic hippocampal rs-FC in the IPL in the discovery, validation, and combined analyses. This novel association of hippocampal-IPL rs-FC with periadolescent memory ability aligns with findings from older adults (Wang et al., 2010) although we did not replicate that study's association of hippocampus-PCC rs-FC with memory. In younger children (ages 4–8 years), differences in hippocampal rs-FC were also related to episodic memory performance, but in different network components including precuneus, vmPFC, and middle temporal gyrus (Geng et al., 2019; Riggins et al., 2016). More broadly, our finding was congruent with prior reports that individual differences in memory are related to strength of rs-FC within the hippocampal/DMN network extent (He et al., 2012; Salami, Pudas, & Nyberg, 2014; Wang et al., 2010; Witte, Kerti, Margulies, & Floel, 2014) often including hippocampus, IPL, and medial PFC. Of note, there was a difference in laterality between the IPL-memory findings for the Dev-CoG dataset (left) and the PNC dataset (right) in the whole-brain analyses, although voxels in the left-lateralized IPL cluster from the Dev-CoG dataset showed the same negative valence in the PNC dataset when tested in a confirmatory ROI analysis. Further, the Dev-CoG cluster remained significant in the combined analysis of the two datasets. Regarding the laterality difference in the whole-brain results, we speculate that this may be attributable to differences in the material to be remembered in the PSMT (verbal and verbalizable stimuli) and PFMT (nonverbalizable face stimuli) based on prior work suggesting left and right temporal lobe specialization for verbal and visual modalities (Kelley et al., 1998; Milner, 1958; Milner, 1972).

The association we observed between hippocampal rs-FC, IPL, and memory ability can also be considered in the context of task-based fMRI studies that have frequently implicated the hippocampus and lateral parietal regions (among others) in active memory processes among children (DeMaster & Ghetti, 2013; Geng et al., 2019; Ofen, Chai, Schuil, Whitfield-Gabrieli, & Gabrieli, 2012), adults (Kim, 2011; Spreng et al., 2009; Svoboda et al., 2006), or both (Tang et al., 2020). For example, negative subsequent memory effects in bilateral supramarginal gyrus were recently reported in a cross-sectional task-based fMRI study of children and adults age 8–25 years (Tang et al., 2020). Further, a parcellation of parietal lobe based on rs-FC analysis of healthy young adults suggested a topology consistent with regional specialization including contributions to memory processes (Nelson et al., 2010). Contributions of parietal lobe to memory processes are also supported by converging evidence from neuropsychological and neurostimulation studies (Berryhill, Phuong, Picasso,

Cabeza, & Olson, 2007; Wang et al., 2014). One interpretation of our finding is that the greater negative covariance we observed between resting activity in the hippocampus and IPL in children with better memory ability represents enhanced segregation of functional brain systems supporting better memory performance and/or general cognitive enhancement; this would be consistent with emerging theoretical accounts of brain development and/or cognitive ability (Chai et al., 2014a; Fair et al., 2007; Fair et al., 2008). Alternatively, IPL could make a regionally specific contribution to certain memory processes (Parvizi & Wagner, 2018; Uncapher, Hutchinson, & Wagner, 2010). Subsequent investigations could disambiguate these possibilities by studying the network using resting-state and task-based fMRI at different developmental stages (Chai, Ofen, Gabrieli, & Whitfield-Gabrieli, 2014b; Geng et al., 2019; Giedd et al., 1996; Gogtay et al., 2006; Ofen et al., 2012; Riggins et al., 2016; Tang et al., 2020).

7.3 | Age and hippocampal rs-FC

We also observed focal covariation between age and hippocampal rs-FC with and without GSR in the discovery dataset, although the patterns differed. With GSR, the age-related left SMG/insula cluster we observed shared valence (positive), laterality (left), and general locale (vicinity of posterior lateral sulcus) with one of several previously reported clusters showing age-related covariance with hippocampal rs-FC in younger children (Blankenship et al., 2017). Of special note for discussion of age-related differences in hippocampal rs-FC, previous work by Blankenship et al. (2017) reported on a sample of 4-to-10-year-old children, but their findings best represented ages 4–8 because 9 and 10 year olds were sparsely sampled (per their Figure 1, approximately three 9 or 10 year olds from $N = 96$). Our study complements the earlier work by reporting age-related changes in hippocampal rs-FC for children 9–15 years old, and our findings suggest that there may be continued age-related changes in hippocampal rs-FC with left SMG/insula from middle childhood through adolescence.

Findings from investigations of age-related differences in DMN are also relevant given the correspondence between rs-FC of hippocampus and DMN. In one study of DMN, age-related changes in IPL regions including supramarginal gyrus were found in a cross-sectional study of ages 8–25, although those changes were right-lateralized and of negative valence (Chai et al., 2014a). Another study of DMN compared the network in children age 8–13 years and young adults (Barber et al., 2013), and those authors reported stronger negative correlations in regions consistent with our observations (albeit more extensive). Notably, the cited studies of DMN have important methodological differences from our study including DMN-specific seed regions, different age ranges, treating age as a discrete factor versus a continuous covariate, and so forth. These differences in implementation may be related to some differences in laterality and valence of age-related differences in IPL across studies. Our findings are consistent with this perspective—while there was significant spatial similarity of age-related differences in hippocampal rs-FC between the

discovery and validation datasets in our study, different focal clusters were identified as significant in the two datasets.

One widely shared finding among analyses of early age-related differences in hippocampal or broader DMN rs-FC is that within-network changes are frequently positive while between-network changes are frequently negative (Barber et al., 2013; Blankenship et al., 2017; Chai et al., 2014b; Dosenbach et al., 2010; Sherman et al., 2014; Supekar et al., 2010). Our findings of age-related covariance followed this general pattern in the discovery and validation datasets. The distinction is evident in the divergence between the anterior and posterior IPL: angular gyrus and supramarginal gyrus showed positive and negative rs-FC with hippocampus, respectively, and their broad age-related trends shared that directionality. In future studies, datasets of greater size may provide sufficient statistical power to elucidate whether positive intranetwork and negative extranetwork changes are a fundamental feature of hippocampal or DMN rs-FC development.

Without GSR, we observed clusters of age-related covariance in right putamen and right IFG. Neither region has been frequently implicated in age-related differences in hippocampal or DMN rs-FC, although left IFG has shown age-related differences as part of a so-called "task-positive" network (Barber et al., 2013).

7.4 | Memory, age, and hippocampal rs-FC

We observed that hippocampal rs-FC exhibited distinct patterns of regional covariance with memory and age. Prior work in younger and older participants has also identified regional covariance with memory and age, but we believe that our study may be the first to report significant covariance of intrinsic functional connectivity of the whole hippocampus with memory and age simultaneously in the same dataset(s). While further investigation is clearly important, our findings prompt questions including: What is the degree of independence between age- and memory-related covariance in hippocampal rs-FC? How does regional covariation with hippocampal rs-FC reflect the contributions of a brain region to brain and cognitive maturation? And does the periadolescent epoch reflect trends evident earlier in development or its own unique pattern?

Regarding the independence of age and memory covariation with hippocampal rs-FC, our findings for the two covariates differed in their valence and in their spatial distribution. Across the discovery and validation datasets, age showed statistically significant regional covariation with hippocampal rs-FC that was both positive and negative, while memory was exclusively associated with negative changes in hippocampal rs-FC. The age-related differences we observed appear to be consistent with prior work suggesting that development is associated with stronger positive rs-FC within intrinsic functional networks and stronger negative rs-FC between networks (Dosenbach et al., 2010; Fair et al., 2007; Fair et al., 2008; Sherman et al., 2014), although these effects have not been previously reported for hippocampal rs-FC in a periadolescent population. Memory-related differences in hippocampal rs-FC are also novel in this population, although

younger and older populations have been reported to show regional variation in hippocampal rs-FC related to memory ability (Geng et al., 2019; Riggins et al., 2016; Wang et al., 2010).

Our observation of concentrated regional covariance effects for memory and age in (distinct) regions of lateral parietal cortex may reflect an important cognitive and developmental relationship with the hippocampus. Structural connectivity between the medial temporal lobes and lateral parietal regions is well-established (Cavada & Goldman-Rakic, 1989; Mesulam, van Hoesen, Pandya, & Geschwind, 1977), and the key white-matter path between these regions (the cingulum) has been reported to develop through early adulthood (Lebel, Walker, Leemans, Phillips, & Beaulieu, 2008; Lebel & Beaulieu, 2011). These developmental changes in brain structure may drive functional segregation of lateral parietal cortex during late childhood and adolescence. At the whole-brain level, network segregation has been associated with maturation (Dosenbach et al., 2010; Fair et al., 2007; Fair et al., 2008) and cognitive ability (Sherman et al., 2014). These findings extend to lateral parietal regions related to memory abilities: in adults, functional segregation of lateral parietal cortex has been described by Nelson et al. (2010) using a parcellation scheme based on resting-state fMRI data that was then interpreted task-based fMRI collected during memory retrieval. The authors identified unique roles in memory (postretrieval monitoring, familiarity judgment, context reinstatement) for different parietal parcels (Nelson et al., 2010). Intriguingly, a parcellation of the same lateral parietal cortex using rs-fMRI data from children (Barnes et al., 2012) replicated many features of the adult parcellation but failed to reproduce a parcel in the anterior inferior parietal lobule (aIPL, near supramarginal gyrus) that had been associated with memory retrieval success/monitoring in adults (Nelson et al., 2010). This aIPL parcel is in close proximity to a region reported by an independent cross-sectional task-based fMRI study of children, adolescents, and young adults (age 8–21 years) which identified a cluster in aIPL/supramarginal gyrus that showed significant activation with retrieval success (hit > miss) which increased with age (Ofen et al., 2012). Intriguingly, the peak of this cluster of activation was located only 6.3 mm from the peak of hippocampal rs-FC covariance with memory that we report here (MNI coordinates X = −56, Y = −50, Z = +36 vs. X = −62, Y = −50, Z = +38). The co-occurrence in this aIPL/supramarginal gyrus region—of age-related differences in the memory retrieval activity in children (Ofen et al., 2012), of child/adult differences in intrinsic organization (Barnes et al., 2012; Nelson et al., 2010), and of covariance of rs-FC with off-line memory ability in periadolescent children (current study)—would be consistent with regionally specific contributions to memory abilities that change during development.

Considered alongside our findings from two periadolescent datasets that memory ability covaried (negatively) with hippocampal rs-FC in supramarginal gyrus, these earlier results may suggest that the development of segregated, regionally specific functional roles within lateral parietal cortex contributes to the maturation of hippocampal-dependent memory abilities—here, supramarginal gyrus/aIPL would play a special role in retrieval monitoring (Barnes et al., 2012; Ofen et al., 2012). Further, it is possible that age and

memory ability may yield dissociable differences in structural/functional connectivity of the hippocampus and lateral parietal cortex. Our account is necessarily speculative, and longitudinal studies of brain and memory development in children and adolescents would be highly informative for this perspective on the developmental relationship between the hippocampus, lateral parietal regions, and memory abilities.

7.5 | Anterior–posterior differences in hippocampal rs-FC

The anterior and posterior hippocampus exhibited overlapping but partly distinct topologies of functional connectivity. Our novel periadolescent findings were consistent with prior work in younger children (Blankenship et al., 2017; Geng et al., 2019; Riggins et al., 2016), adults (Hrybouski et al., 2019; Poppenk & Moscovitch, 2011; Qin et al., 2016; Ranganath & Ritchey, 2012), or both (Tang et al., 2020). Specifically, we observed that posterior hippocampus exhibited stronger rs-FC with precuneus, posterior cingulate, and anterior cingulate regions; anterior hippocampus exhibited stronger rs-FC with paracentral lobule and other somatomotor regions. This pattern was consistent with a previous graph-theoretic characterization of anterior and posterior hippocampal rs-FC which observed that posterior hippocampus exhibited stronger and broader connectivity than anterior hippocampus (Qin et al., 2016). Notably, the set of regions identified in our analysis was less spatially extensive than reported in studies of younger children (Blankenship et al., 2017; Riggins et al., 2016). For example, we did not observe significantly greater rs-FC between anterior hippocampus and medial PFC/frontopolar regions, although there was nonsignificant numerical evidence of similar patterns. This could be attributable to age-related differences in long-axis specialization of the hippocampus—supporting this perspective, Poppenk and Moscovitch (2011) studied hippocampal rs-FC in adults and did not report that anterior hippocampus showed stronger rs-FC with medial PFC. Similarly, analysis of rs-FC for medial temporal lobe neocortical regions adjacent to hippocampus in adults suggests that posterior MTL regions (parahippocampal cortex) have greater rs-FC with medial PFC than anterior regions (Ranganath & Ritchey, 2012). Finally, we did not observe significant covariance of anterior or posterior hippocampal rs-FC with age or memory. Although further analysis of differences in anterior–posterior hippocampal rs-FC were beyond the scope of our study, subsequent investigations could test for age-related differences in anterior–posterior hippocampal rs-FC by sampling from child, adolescent, and young adult populations with a consistent neuroimaging approach.

7.6 | Limitations

Our study had some limitations. Regarding neuroimaging data from the Dev-CoG dataset, we collected two 5-min resting-state fMRI recordings from each participant, but the recordings used slightly

different instructions (i.e., eyes-open vs. eyes-closed). We included EPI data recorded under both instruction sets in the current study to maximize the amount of data retained after censoring and thereby enhance the reliability of our rs-FC estimates (Birn et al., 2013). We acknowledge that including data from both conditions may have influenced rs-FC patterns (Agcaoglu, Wilson, Wang, Stephen, & Calhoun, 2019; Patriat et al., 2013). However, our functional data were evenly balanced between the two rest conditions during collection by design, and our findings were broadly consistent with prior work on hippocampal rs-FC in children and adults (Blankenship et al., 2017; Kahn et al., 2008; Riggins et al., 2016; Riggins et al., 2016; Vincent et al., 2006). Further, we explicitly contrasted the eyes-open and eyes-open conditions in a supporting analysis, and the limited differences were concentrated in regions not found to be statistically significant in other analyses. Also relevant to the neuroimaging data, our youth sample included many participants who exhibited in-scanner motion typical for the age range (Dosenbach et al., 2017; Power et al., 2012; Satterthwaite et al., 2012). We addressed this by applying best practice recommendations for attenuating artifactual effects of motion on rs-FC analysis including censoring of high-motion fMRI volumes, regression of realignment parameters and derivatives, and exclusion of participants with excessive motion (Power et al., 2012; Power, Mitra, et al., 2014; Satterthwaite et al., 2012). We believe that these measures adequately controlled nuisance effects related to motion in our study.

Another limitation of our study was that the sampled age range in the discovery and validation datasets was constrained to 9–15 years in order to fill a gap in the literature regarding hippocampal rs-FC in the periadolescent epoch. This design choice did not afford the opportunity to test whether the observed effects were specific to the periadolescent epoch, although we identified differences between our findings and prior reports describing younger and older participants. Rigorous analysis of the full developmental trajectory of hippocampal rs-FC could be robustly addressed by future studies sampling a wider age range (Lenroot & Giedd, 2006; Ofen et al., 2012). Finally, there were substantial differences in the MRI scan parameters, scan durations, and cognitive assessments in the discovery (Dev-CoG) and validation (PNC) datasets. We note that despite these differences, we observed many striking similarities in overall hippocampal rs-FC and covariation with other variables between the individual datasets and in our combined analysis. To the extent that the datasets differed in certain aspects of data collection, our frequent observation of effects common to both datasets (e.g., covariance of hippocampal rs-FC with age and memory) suggests robust, reproducible characteristics of the intrinsic functional connectivity of the hippocampus.

8 | CONCLUSIONS

We observed a pattern of hippocampal rs-FC in periadolescent children that represents a novel observation on the developmental continuum between prior studies of this brain network in younger and older populations. Our findings bridge a gap in the current literature

by demonstrating that while periadolescent hippocampal rs-FC resembles that of young children and adults, associations with certain network components such as the middle temporal gyrus may change during development. In support of this perspective, we found evidence of regional covariance of hippocampal rs-FC with participant age. Additionally, we observed focal differences in hippocampal rs-FC associated with hippocampal-dependent memory ability in lateral parietal regions (supramarginal gyrus) that were novel in a periadolescent population and suggestive of a developmental trajectory for functional brain networks supporting relational memory processes. Taken together, our observations are consistent with a developmental trajectory for hippocampal rs-FC that extends through at least early adolescence. Future studies might evaluate whether the same patterns are observed longitudinally, and whether this developmental course is affected by genetic, hormonal, or environmental factors. Further study of functional development of the hippocampus and its intrinsic connectivity is warranted due to the relevance of the hippocampus to lifespan neurological and psychiatric health as well as the structure's central role in the childhood development of memory abilities.

CONFLICT OF INTERESTS

The authors declare no conflict of interests.

AUTHOR CONTRIBUTIONS

All authors designed the research. **Tony W. Wilson**, **Vince D. Calhoun**, and **Julia M. Stephen**: Supervised data collection. **David E. Warren**: Performed the analyses. All authors wrote the paper.

DATA AVAILABILITY STATEMENT

The data that support the findings of this study are available from the principal investigators of the Dev-CoG project upon request.

ORCID

David E. Warren https://orcid.org/0000-0003-0539-2587
Tony W. Wilson https://orcid.org/0000-0002-5053-8306

REFERENCES

Agcaoglu, O., Wilson, T. W., Wang, Y., Stephen, J., & Calhoun, V. D. (2019). Resting state connectivity differences in eyes open versus eyes closed conditions. *Human Brain Mapping*, 40, 2488–2498.

Andrews-Hanna, J. R., Snyder, A. Z., Vincent, J. L., Lustig, C., Head, D., Raichle, M. E., & Buckner, R. L. (2007). Disruption of large-scale brain systems in advanced aging. *Neuron*, 56, 924–935.

Avants, B. B., Tustison, N. J., Wu, J., Cook, P. A., & Gee, J. C. (2011). An open source multivariate framework for n-tissue segmentation with evaluation on public data. *Neuroinformatics*, 9, 381–400.

Barber, A. D., Caffo, B. S., Pekar, J. J., & Mostofsky, S. H. (2013). Developmental changes in within- and between-network connectivity between late childhood and adulthood. *Neuropsychologia*, 51, 156–167.

Barnes, K. A., Nelson, S. M., Cohen, A. L., Power, J. D., Coalson, R. S., Miezin, F. M., ... Schlaggar, B. L. (2012). Parcellation in left lateral parietal cortex is similar in adults and children. *Cerebral Cortex*, 22, 1148–1158.

Berryhill, M. E., Phuong, L., Picasso, L., Cabeza, R., & Olson, I. R. (2007). Parietal lobe and episodic memory: Bilateral damage causes impaired free recall of autobiographical memory. *Journal of Neuroscience*, 27, 14415–14423.

Birn, R. M., Molloy, E. K., Patriat, R., Parker, T., Meier, T. B., Kirk, G. R., ... Prabhakaran, V. (2013). The effect of scan length on the reliability of resting-state fMRI connectivity estimates. *NeuroImage*, 83, 550–558.

Biswal, B., Zerrin Yetkin, F., Haughton, V. M., & Hyde, J. S. (1995). Functional connectivity in the motor cortex of resting human brain using echo-planar MRI. *Magnetic Resonance in Medicine*, 34, 537–541.

Blankenship, S. L., Redcay, E., Dougherty, L. R., & Riggins, T. (2017). Development of hippocampal functional connectivity during childhood: Hippocampal functional connectivity development. *Human Brain Mapping*, 38, 182–201.

Brainerd, C. J., Stein, L. M., & Reyna, V. F. (1998). On the development of conscious and unconscious memory. *Developmental Psychology*, 34, 342–357.

Buckner, R. L., Andrews-Hanna, J. R., & Schacter, D. L. (2008). The brain's default network: Anatomy, function, and relevance to disease. *Annals of the New York Academy of Sciences*, 1124, 1–38.

Carrion, V. G., Weems, C. F., & Reiss, A. L. (2007). Stress predicts brain changes in children: A pilot longitudinal study on youth stress, posttraumatic stress disorder, and the hippocampus. *Pediatrics*, 119, 509–516.

Cavada, C., & Goldman-Rakic, P. S. (1989). Posterior parietal cortex in rhesus monkey: I. Parcellation of areas based on distinctive limbic and sensory corticocortical connections. *Journal of Comparative Neurology*, 287, 393–421.

Chai, X. J., Ofen, N., Gabrieli, J. D. E., & Whitfield-Gabrieli, S. (2014a). Selective development of anticorrelated networks in the intrinsic functional organization of the human brain. *Journal of Cognitive Neuroscience*, 26, 501–513.

Chai, X. J., Ofen, N., Gabrieli, J. D. E., & Whitfield-Gabrieli, S. (2014b). Development of deactivation of the default-mode network during episodic memory formation. *NeuroImage*, 84, 932–938.

Ciric, R., Wolf, D. H., Power, J. D., Roalf, D. R., Baum, G. L., Ruparel, K., ... Satterthwaite, T. D. (2017). Benchmarking of participant-level confound regression strategies for the control of motion artifact in studies of functional connectivity. *NeuroImage*, 154, 174–187.

Cohen, N. J., & Squire, L. R. (1980). Preserved learning and retention of pattern-analyzing skill in amnesia: Dissociation of knowing how and knowing that. *Science*, 210, 207–210.

Cox, R. W. (1996). AFNI: Software for analysis and visualization of functional magnetic resonance neuroimages. *Computers and Biomedical Research*, 29, 162–173.

Cox, R. W., Chen, G., Glen, D. R., Reynolds, R. C., & Taylor, P. A. (2017). FMRI clustering in AFNI: False-positive rates Redux. *Brain Connectivity*, 7, 152–171.

Dahl, R. E. (2004). Adolescent brain development: A period of vulnerabilities and opportunities. Keynote Address. *Annals of the New York Academy of Sciences*, 1021, 1–22.

Damoiseaux, J. S. (2012). Resting-state fMRI as a biomarker for Alzheimer's disease? *Alzheimer's Research & Therapy*, 4, 8.

DeMaster, D., Pathman, T., Lee, J. K., & Ghetti, S. (2014). Structural development of the hippocampus and episodic memory: Developmental differences along the anterior/posterior axis. *Cerebral Cortex*, *24*, 3036–3045.

DeMaster, D. M., & Ghetti, S. (2013). Developmental differences in hippocampal and cortical contributions to episodic retrieval. *Cortex*, *49*, 1482–1493.

Dice, L. R. (1945). Measures of the amount of ecologic association between species. *Ecology*, *26*, 297–302.

Dikmen, S. S., Bauer, P. J., Weintraub, S., Mungas, D., Slotkin, J., Beaumont, J. L., ... Heaton, R. K. (2014). Measuring episodic memory across the lifespan: NIH Toolbox Picture Sequence Memory Test. *Journal of the International Neuropsychological Society*, *20*, 611–619.

Dosenbach, N. U. F., Koller, J. M., Earl, E. A., Miranda-Dominguez, O., Klein, R. L., Van, A. N., ... Fair, D. A. (2017). Real-time motion analytics during brain MRI improve data quality and reduce costs. *NeuroImage* Retrieved from http://linkinghub.elsevier.com/retrieve/pii/S1053811917306729, *161*, 80–93.

Dosenbach, N. U. F., Nardos, B., Cohen, A. L., Fair, D. A., Power, J. D., Church, J. A., ... Schlaggar, B. L. (2010). Prediction of individual brain maturity using fMRI. *Science (New York, NY)*, *329*, 1358–1361.

Duvernoy, H. M. (2005). *The human hippocampus: Functional anatomy, vascularization, and serial sections with MRI* (3rd ed.). Berlin: Springer.

Eichenbaum, H., & Cohen, N. J. (2001). *From conditioning to conscious recollection: Memory systems of the brain*. New York, NY: Oxford University Press.

Eklund, A., Knutsson, H., & Nichols, T. E. (2018). Cluster failure revisited: Impact of first level design and data quality on cluster false positive rates. *Human Brain Mapping*, *40*, 2017–2032. https://doi.org/10.1002/hbm.24350

Eklund, A., Nichols, T. E., & Knutsson, H. (2016). Cluster failure: Why fMRI inferences for spatial extent have inflated false-positive rates. *Proceedings of the National Academy of Sciences of the United States of America*, *113*, 7900–7905.

Faghiri, A., Stephen, J. M., Wang, Y.-P., Wilson, T. W., & Calhoun, V. D. (2017). Changing brain connectivity dynamics: From early childhood to adulthood. *Human Brain Mapping*, *39*, 1108–1117. https://doi.org/10.1002/hbm.23896

Fair, D. A., Cohen, A. L., Dosenbach, N. U. F., Church, J. A., Miezin, F. M., Barch, D. M., ... Schlaggar, B. L. (2008). The maturing architecture of the brain's default network. *Proceedings of the National Academy of Sciences of the United States of America*, *105*, 4028–4032.

Fair, D. A., Dosenbach, N. U. F., Church, J. A., Cohen, A. L., Brahmbhatt, S., Miezin, F. M., ... Schlaggar, B. L. (2007). Development of distinct control networks through segregation and integration. *Proceedings of the National Academy of Sciences of the United States of America*, *104*, 13507–13512.

Finn, A. S., Kalra, P. B., Goetz, C., Leonard, J. A., Sheridan, M. A., & Gabrieli, J. D. E. (2016). Developmental dissociation between the maturation of procedural memory and declarative memory. *Journal of Experimental Child Psychology*, *142*, 212–220.

Fischl, B. (2004). Automatically parcellating the human cerebral cortex. *Cerebral Cortex*, *14*, 11–22.

Fonov, V., Evans, A. C., Botteron, K., Almli, C. R., McKinstry, R. C., Collins, D. L., & Brain Development Cooperative Group. (2011). Unbiased average age-appropriate atlases for pediatric studies. *NeuroImage*, *54*, 313–327.

Fonov, V. S., Evans, A. C., McKinstry, R. C., Almli, C. R., & Collins, D. L. (2009). Unbiased nonlinear average age-appropriate brain templates from birth to adulthood. *NeuroImage*, *47*, S102 Retrieved from http://linkinghub.elsevier.com/retrieve/pii/S1053811909708845

Fox, M. D., Snyder, A. Z., Vincent, J. L., Corbetta, M., Van Essen, D. C., & Raichle, M. E. (2005). The human brain is intrinsically organized into dynamic, anticorrelated functional networks. *Proceedings of the National Academy of Sciences of the United States of America*, *102*, 9673–9678.

Fox, M. D., Zhang, D., Snyder, A. Z., & Raichle, M. E. (2009). The global signal and observed anticorrelated resting state brain networks. *Journal of Neurophysiology*, *101*, 3270–3283.

Gazzaley, A., Rissman, J., & D'Esposito, M. (2004). Functional connectivity during working memory maintenance. *Cognitive, Affective, & Behavioral Neuroscience*, *4*, 580–599.

Geng, F., Redcay, E., & Riggins, T. (2019). The influence of age and performance on hippocampal function and the encoding of contextual information in early childhood. *NeuroImage*, *195*, 433–443.

Ghetti, S., & Bunge, S. A. (2012). Neural changes underlying the development of episodic memory during middle childhood. *Developmental Cognitive Neuroscience*, *2*, 381–395.

Ghetti, S., DeMaster, D. M., Yonelinas, A. P., & Bunge, S. A. (2010). Developmental differences in medial temporal lobe function during memory encoding. *Journal of Neuroscience*, *30*, 9548–9556.

Giedd, J. N. (2008). The teen brain: Insights from neuroimaging. *Journal of Adolescent Health*, *42*, 335–343.

Giedd, J. N., Vaituzis, A. C., Hamburger, S. D., Lange, N., Rajapakse, J. C., Kaysen, D., ... Rapoport, J. L. (1996). Quantitative MRI of the temporal lobe, amygdala, and hippocampus in normal human development: Ages 4–18 years. *Journal of Comparative Neurology*, *366*, 223–230.

Gogtay, N., Nugent, T. F., Herman, D. H., Ordonez, A., Greenstein, D., Hayashi, K. M., ... Thompson, P. M. (2006). Dynamic mapping of normal human hippocampal development. *Hippocampus*, *16*, 664–672.

Hannula, D. E., Ryan, J. D., Tranel, D., & Cohen, N. J. (2007). Rapid onset relational memory effects are evident in eye movement behavior, but not in hippocampal amnesia. *Journal of Cognitive Neuroscience*, *19*, 1690–1705.

Hannula, D. E., Tranel, D., & Cohen, N. J. (2006). The long and the short of it: Relational memory impairments in amnesia, even at short lags. *The Journal of Neuroscience*, *26*, 8352–8359.

Hanson, J. L., Nacewicz, B. M., Sutterer, M. J., Cayo, A. A., Schaefer, S. M., Rudolph, K. D., ... Davidson, R. J. (2015). Behavioral problems after early life stress: Contributions of the hippocampus and amygdala. *Biological Psychiatry*, *77*, 314–323.

Hare, S. M., Law, A. S., Ford, J. M., Mathalon, D. H., Ahmadi, A., Damaraju, E., ... Turner, J. A. (2018). Disrupted network cross talk, hippocampal dysfunction and hallucinations in schizophrenia. *Schizophrenia Research*, *199*, 226–234.

He, J., Carmichael, O., Fletcher, E., Singh, B., Iosif, A.-M., Martinez, O., ... Decarli, C. (2012). Influence of functional connectivity and structural MRI measures on episodic memory. *Neurobiology of Aging*, *33*, 2612–2620. http://www.ncbi.nlm.nih.gov/pubmed/22285758

Hohenfeld, C., Werner, C. J., & Reetz, K. (2018). Resting-state connectivity in neurodegenerative disorders: Is there potential for an imaging biomarker? *NeuroImage: Clinical*, *18*, 849–870.

Hrybouski, S., MacGillivray, M., Huang, Y., Madan, C. R., Carter, R., Seres, P., & Malykhin, N. V. (2019). Involvement of hippocampal subfields and anterior-posterior subregions in encoding and retrieval of item, spatial, and associative memories: Longitudinal versus transverse axis. *NeuroImage*, *191*, 568–586.

Insausti, R., Juottonen, K., Soininen, H., Insausti, A. M., Partanen, K., Vainio, P., ... Pitkänen, A. (1998). MR volumetric analysis of the human entorhinal, perirhinal, and temporopolar cortices. *AJNR American Journal of Neuroradiology*, *19*, 659–671.

Jackowski, A. P., de Araújo, C. M., de Lacerda, A. L. T., de Jesus, M. J., & Kaufman, J. (2009). Neurostructural imaging findings in children with post-traumatic stress disorder: Brief review. *Psychiatry and Clinical Neurosciences*, *63*, 1–8.

Joëls, M. (2009). Stress, the hippocampus, and epilepsy. *Epilepsia*, *50*, 586–597.

Johnson, M. H. (2001). Functional brain development in humans. *Nature Reviews. Neuroscience*, *2*, 475–483.

Kahn, I., Andrews-Hanna, J. R., Vincent, J. L., Snyder, A. Z., & Buckner, R. L. (2008). Distinct cortical anatomy linked to subregions of the medial temporal lobe revealed by intrinsic functional connectivity. *Journal of Neurophysiology*, *100*, 129–139.

Kelley, W. M., Miezin, F. M., McDermott, K. B., Buckner, R. L., Raichle, M. E., Cohen, N. J., … Petersen, S. E. (1998). Hemispheric specialization in human dorsal frontal cortex and medial temporal lobe for verbal and nonverbal memory encoding. *Neuron*, *20*, 927–936.

Kim, H. (2011). Neural activity that predicts subsequent memory and forgetting: A meta-analysis of 74 fMRI studies. *NeuroImage*, *54*, 2446–2461.

Lebel, C., & Beaulieu, C. (2011). Longitudinal development of human brain wiring continues from childhood into adulthood. *Journal of Neuroscience*, *31*, 10937–10947.

Lebel, C., Walker, L., Leemans, A., Phillips, L., & Beaulieu, C. (2008). Microstructural maturation of the human brain from childhood to adulthood. *NeuroImage*, *40*, 1044–1055.

Lee, J. K., Wendelken, C., Bunge, S. A., & Ghetti, S. (2016). A time and place for everything: Developmental differences in the building blocks of episodic memory. *Child Development*, *87*, 194–210.

Lenroot, R. K., & Giedd, J. N. (2006). Brain development in children and adolescents: Insights from anatomical magnetic resonance imaging. *Neuroscience & Biobehavioral Reviews*, *30*, 718–729.

Li, X., Morgan, P. S., Ashburner, J., Smith, J., & Rorden, C. (2016). The first step for neuroimaging data analysis: DICOM to NIfTI conversion. *Journal of Neuroscience Methods*, *264*, 47–56.

MacMaster, F. P., & Kusumakar, V. (2004). Hippocampal volume in early onset depression. *BMC Medicine*, *2*, 2.

Menon, V. (2013). Developmental pathways to functional brain networks: Emerging principles. *Trends in Cognitive Sciences*, *17*, 627–640.

Mesulam, M.-M., van Hoesen, G. W., Pandya, D. N., & Geschwind, N. (1977). Limbic and sensory connections of the inferior parietal lobule (area PG) in the rhesus monkey: A study with a new method for horseradish peroxidase histochemistry. *Brain Research*, *136*, 393–414.

Milner, B. (1958). Psychological defects produced by temporal lobe excision. *Research Publications - Association for Research in Nervous and Mental Disease*, *36*, 244–257.

Milner, B. (1972). Disorders of learning and memory after temporal lobe lesions in man. *Clinical Neurosurgery*, *19*, 421–446.

Mohamed, A., Wyllie, E., Ruggieri, P., Kotagal, P., Babb, T., Hilbig, A., … Bingaman, W. (2001). Temporal lobe epilepsy due to hippocampal sclerosis in pediatric candidates for epilepsy surgery. *Neurology*, *56*, 1643–1649.

Moore, T. M., Reise, S. P., Gur, R. E., Hakonarson, H., & Gur, R. C. (2015). Psychometric properties of the Penn computerized neurocognitive battery. *Neuropsychology*, *29*, 235–246.

Murphy, K., & Fox, M. D. (2017). Towards a consensus regarding global signal regression for resting state functional connectivity MRI. *NeuroImage*, *154*, 169–173.

Nelson, S. M., Cohen, A. L., Power, J. D., Wig, G. S., Miezin, F. M., Wheeler, M. E., … Petersen, S. E. (2010). A parcellation scheme for human left lateral parietal cortex. *Neuron*, *67*, 156–170.

Nielsen, A. N., Greene, D. J., Gratton, C., Dosenbach, N. U. F., Petersen, S. E., & Schlaggar, B. L. (2019). Evaluating the prediction of brain maturity from functional connectivity after motion artifact denoising. *Cerebral Cortex*, *29*, 2455–2469.

Noble, S., Scheinost, D., & Constable, R. T. (2019). A decade of test-retest reliability of functional connectivity: A systematic review and meta-analysis. *NeuroImage*, *203*, 116157.

Ofen, N. (2012). The development of neural correlates for memory formation. *Neuroscience & Biobehavioral Reviews*, *36*, 1708–1717.

Ofen, N., Chai, X. J., Schuil, K. D. I., Whitfield-Gabrieli, S., & Gabrieli, J. D. E. (2012). The development of brain systems associated with successful memory retrieval of scenes. *Journal of Neuroscience*, *32*, 10012–10020.

Ofen, N., Kao, Y.-C., Sokol-Hessner, P., Kim, H., Whitfield-Gabrieli, S., & Gabrieli, J. D. E. (2007). Development of the declarative memory system in the human brain. *Nature Neuroscience*, *10*, 1198–1205.

Olson, I. R., & Newcombe, N. S. (2014). Binding together the elements of episodes: Relational memory and the developmental trajectory of the hippocampus. In *The Wiley handbook on the development of children's memory*. (pp. 285–308). Hoboken, NJ: Wiley Blackwell.

Overman, W. H., Pate, B. J., Moore, K., & Peuster, A. (1996). Ontogeny of place learning in children as measured in the radial arm maze, Morris search task, and open field task. *Behavioral Neuroscience*, *110*, 1205–1228.

Parvizi, J., & Wagner, A. D. (2018). Memory, numbers, and action decision in human posterior parietal cortex. *Neuron*, *97*, 7–10.

Patriat, R., Molloy, E. K., Meier, T. B., Kirk, G. R., Nair, V. A., Meyerand, M. E., … Birn, R. M. (2013). The effect of resting condition on resting-state fMRI reliability and consistency: A comparison between resting with eyes open, closed, and fixated. *NeuroImage*, *78*, 463–473.

Poldrack, R. A., Baker, C. I., Durnez, J., Gorgolewski, K. J., Matthews, P. M., Munafò, M. R., … Yarkoni, T. (2017). Scanning the horizon: Towards transparent and reproducible neuroimaging research. *Nature Reviews Neuroscience*, *18*, 115–126. https://doi.org/10.1038/nrn.2016.167

Poppenk, J., & Moscovitch, M. (2011). A hippocampal marker of recollection memory ability among healthy young adults: Contributions of posterior and anterior segments. *Neuron*, *72*, 931–937.

Power, J. D., Barnes, K. A., Snyder, A. Z., Schlaggar, B. L., & Petersen, S. E. (2012). Spurious but systematic correlations in functional connectivity MRI networks arise from subject motion. *NeuroImage*, *59*, 2142–2154.

Power, J. D., Cohen, A. L., Nelson, S. M., Wig, G. S., Barnes, K. A., Church, J. A., … Petersen, S. E. (2011). Functional network organization of the human brain. *Neuron*, *72*, 665–678.

Power, J. D., Mitra, A., Laumann, T. O., Snyder, A. Z., Schlaggar, B. L., & Petersen, S. E. (2014). Methods to detect, characterize, and remove motion artifact in resting state fMRI. *NeuroImage*, *84*, 320–341.

Power, J. D., Schlaggar, B. L., & Petersen, S. E. (2014). Recent progress and outstanding issues in motion correction in resting state fMRI. *NeuroImage*, *105*, 536–551. https://doi.org/10.1016/j.neuroimage.2014.10.044

Qin, S., Duan, X., Supekar, K., Chen, H., Chen, T., & Menon, V. (2016). Large-scale intrinsic functional network organization along the long axis of the human medial temporal lobe. *Brain Structure & Function*, *221*, 3237–3258.

Raichle, M. E., Macleod, A. M., Snyder, A. Z., Powers, W. J., Gusnard, D. A., & Shulman, G. L. (2001). A default mode of brain function. *Proceedings of the National Academy of Sciences of the United States of America*, *98*, 676–682.

Ranganath, C. (2010). A unified framework for the functional organization of the medial temporal lobes and the phenomenology of episodic memory. *Hippocampus*, *20*, 1263–1290.

Ranganath, C., & D'Esposito, M. (2001). Medial temporal lobe activity associated with active maintenance of novel information. *Neuron*, *31*, 865–873.

Ranganath, C., & Ritchey, M. (2012). Two cortical systems for memory-guided behaviour. *Nature Reviews Neuroscience*, *13*, 713–726.

Riggins, T., Geng, F., Blankenship, S. L., & Redcay, E. (2016). Hippocampal functional connectivity and episodic memory in early childhood. *Developmental Cognitive Neuroscience*, *19*, 58–69.

Salami, A., Pudas, S., & Nyberg, L. (2014). Elevated hippocampal resting-state connectivity underlies deficient neurocognitive function in aging. *Proceedings of the National Academy of Sciences of the United States of America*, *111*, 17654–17659.

Satterthwaite, T. D., Connolly, J. J., Ruparel, K., Calkins, M. E., Jackson, C., Elliott, M. A., … Gur, R. E. (2016). The Philadelphia Neurodevelopmental Cohort: A publicly available resource for the study of normal and abnormal brain development in youth. *NeuroImage*, *124*, 1115–1119.

Satterthwaite, T. D., Elliott, M. A., Gerraty, R. T., Ruparel, K., Loughead, J., Calkins, M. E., … Wolf, D. H. (2013). An improved framework for confound regression and filtering for control of motion artifact in the preprocessing of resting-state functional connectivity data. *NeuroImage*, *64*, 240–256.

Satterthwaite, T. D., Elliott, M. A., Ruparel, K., Loughead, J., Prabhakaran, K., Calkins, M. E., … Gur, R. E. (2014). Neuroimaging of the Philadelphia neurodevelopmental cohort. *NeuroImage*, *86*, 544–553.

Satterthwaite, T. D., Wolf, D. H., Loughead, J., Ruparel, K., Elliott, M. A., Hakonarson, H., ... Gur, R. E. (2012). Impact of in-scanner head motion on multiple measures of functional connectivity: Relevance for studies of neurodevelopment in youth. *NeuroImage, 60*, 623–632.

Schneider, W., Bjorklund, D., & Valsiner, J. (2003). Memory and knowledge development. In J. Valsiner & K. Connolly (Eds.), *Handbook of Developmental Psychology* (pp. 370–403). Thousand Oaks, CA: SAGE Publications.

Scoville, W. B., & Milner, B. (1957). Loss of recent memory after bilateral hippocampal lesions. *Journal of Neurology, Neurosurgery, and Psychiatry, 20*, 11–21.

Sherman, L. E., Rudie, J. D., Pfeifer, J. H., Masten, C. L., McNealy, K., & Dapretto, M. (2014). Development of the default mode and central executive networks across early adolescence: A longitudinal study. *Developmental Cognitive Neuroscience, 10*, 148–159.

Slotkin, J., Kallen, M., Griffith, J., Magasi, S., Salsman, H., Nowinski, C., & Gershon, R. (2012). *NIH toolbox technical manual*. Bethesda, MD: National Institutes of Health.

Sowell, E. R., Delis, D., Stiles, J., & Jernigan, T. L. (2001). Improved memory functioning and frontal lobe maturation between childhood and adolescence: A structural MRI study. *Journal of the International Neuropsychological Society, 7*, 312–322.

Spreng, R. N., Mar, R. A., & Kim, A. S. N. (2009). The common neural basis of autobiographical memory, prospection, navigation, theory of mind, and the default mode: A quantitative meta-analysis. *Journal of Cognitive Neuroscience, 21*, 489–510.

Stephen, J. M., Solis, I., Janowich, J., Stern, M., Frenzel, M. R., Eastman, J. A., ... Calhoun, V. D. (2021). The Developmental Chronnecto-Genomics (Dev-CoG) study: A multimodal study on the developing brain. *NeuroImage, 225*, 117438.

Stevens, M. C., Pearlson, G. D., & Calhoun, V. D. (2009). Changes in the interaction of resting-state neural networks from adolescence to adulthood. *Human Brain Mapping, 30*, 2356–2366.

Supekar, K., Uddin, L. Q., Prater, K., Amin, H., Greicius, M. D., & Menon, V. (2010). Development of functional and structural connectivity within the default mode network in young children. *NeuroImage, 52*, 290–301.

Svoboda, E., McKinnon, M. C., & Levine, B. (2006). The functional neuroanatomy of autobiographical memory: A meta-analysis. *Neuropsychologia, 44*, 2189–2208.

Tang, L., Pruitt, P. J., Yu, Q., Homayouni, R., Daugherty, A. M., Damoiseaux, J. S., & Ofen, N. (2020). Differential functional connectivity in anterior and posterior hippocampus supporting the development of memory formation. *Frontiers in Human Neuroscience, 14*, 204.

Taylor, P. A., Chen, G., Glen, D. R., Rajendra, J. K., Reynolds, R. C., & Cox, R. W. (2018). FMRI processing with AFNI: Some comments and corrections on "exploring the impact of analysis software on task fMRI results". *Neuroscience*. https://doi.org/10.1101/308643

Tulsky, D. S., Carlozzi, N., Chiaravalloti, N. D., Beaumont, J. L., Kisala, P. A., Mungas, D., ... Gershon, R. (2014). NIH Toolbox Cognition Battery (NIHTB-CB): List sorting test to measure working memory. *Journal of the International Neuropsychological Society, 20*, 599–610.

Tustison, N. J., Avants, B. B., Cook, P. A., Zheng, Y., Egan, A., Yushkevich, P. A., & Gee, J. C. (2010). N4ITK: Improved N3 bias correction. *IEEE Transactions on Medical Imaging, 29*, 1310–1320.

Uddin, L. Q., Supekar, K., & Menon, V. (2010). Typical and atypical development of functional human brain networks: Insights from resting-state FMRI. *Frontiers in Systems Neuroscience, 4*, 21.

Uecker, A., & Nadel, L. (1996). Spatial locations gone awry: Object and spatial memory deficits in children with fetal alcohol syndrome. *Neuropsychologia, 34*, 209–223.

Uncapher, M. R., Hutchinson, J. B., & Wagner, A. D. (2010). A roadmap to brain mapping: Toward a functional map of human parietal cortex. *Neuron, 67*, 5–8.

van Erp, T. G. M., Hibar, D. P., Rasmussen, J. M., Glahn, D. C., Pearlson, G. D., Andreassen, O. A., ... Turner, J. A. (2016). Subcortical brain volume abnormalities in 2028 individuals with schizophrenia and 2540 healthy controls via the ENIGMA consortium. *Molecular Psychiatry, 21*, 547–553.

Vincent, J. L., Snyder, A. Z., Fox, M. D., Shannon, B. J., Andrews, J. R., Raichle, M. E., & Buckner, R. L. (2006). Coherent spontaneous activity identifies a hippocampal-parietal memory network. *Journal of Neurophysiology, 96*, 3517–3531.

Volkow, N. D., Koob, G. F., Croyle, R. T., Bianchi, D. W., Gordon, J. A., Koroshetz, W. J., ... Weiss, S. R. B. (2018). The conception of the ABCD study: From substance use to a broad NIH collaboration. *Developmental Cognitive Neuroscience, 32*, 4–7.

Wang, J. X., Rogers, L. M., Gross, E. Z., Ryals, A. J., Dokucu, M. E., Brandstatt, K. L., ... Voss, J. L. (2014). Targeted enhancement of cortical-hippocampal brain networks and associative memory. *Science, 345*, 1054–1057.

Wang, L., LaViolette, P., O'Keefe, K., Putcha, D., Bakkour, A., van Dijk, K. R. A., ... Sperling, R. A. (2010). Intrinsic connectivity between the hippocampus and posteromedial cortex predicts memory performance in cognitively intact older individuals. *NeuroImage, 51*, 910–917.

Ward, A. M., Schultz, A. P., Huijbers, W., van Dijk, K. R. A., Hedden, T., & Sperling, R. A. (2014). The parahippocampal gyrus links the default-mode cortical network with the medial temporal lobe memory system: DMN-MTL connectivity. *Human Brain Mapping, 35*, 1061–1073.

Warren, D. E., Duff, M. C., Jensen, U., Tranel, D., & Cohen, N. J. (2012). Hiding in plain view: Lesions of the medial temporal lobe impair online representation. *Hippocampus, 22*, 1577–1588.

Watson, P. D., Voss, J. L., Warren, D. E., Tranel, D., & Cohen, N. J. (2013). Spatial reconstruction by patients with hippocampal damage is dominated by relational memory errors. *Hippocampus, 23*, 570–580.

Weintraub, S., Dikmen, S. S., Heaton, R. K., Tulsky, D. S., Zelazo, P. D., Bauer, P. J., ... Gershon, R. C. (2013). Cognition assessment using the NIH Toolbox. *Neurology, 80*, S54–S64.

Winkler, A. M., Webster, M. A., Brooks, J. C., Tracey, I., Smith, S. M., & Nichols, T. E. (2016). Non-parametric combination and related permutation tests for neuroimaging: NPC and related permutation tests for neuroimaging. *Human Brain Mapping, 37*, 1486–1511.

Winterburn, J. L., Pruessner, J. C., Chavez, S., Schira, M. M., Lobaugh, N. J., Voineskos, A. N., & Chakravarty, M. M. (2013). A novel in vivo atlas of human hippocampal subfields using high-resolution 3 T magnetic resonance imaging. *NeuroImage, 74*, 254–265.

Witte, A. V., Kerti, L., Margulies, D. S., & Floel, A. (2014). Effects of resveratrol on memory performance, hippocampal functional connectivity, and glucose metabolism in healthy older adults. *Journal of Neuroscience, 34*, 7862–7870.

Zhang, D., & Raichle, M. E. (2010). Disease and the brain's dark energy. *Nature Reviews. Neurology, 6*, 15–28.

Zhou, Y., Shu, N., Liu, Y., Song, M., Hao, Y., Liu, H., ... Jiang, T. (2008). Altered resting-state functional connectivity and anatomical connectivity of hippocampus in schizophrenia. *Schizophrenia Research, 100*, 120–132.

SUPPORTING INFORMATION

Additional supporting information may be found online in the Supporting Information section at the end of this article.

How to cite this article: Warren, D. E., Rangel, A. J., Christopher-Hayes, N. J., Eastman, J. A., Frenzel, M. R., Stephen, J. M., Calhoun, V. D., Wang, Y.-P., Wilson, T. W. (2021). Resting-state functional connectivity of the human hippocampus in periadolescent children: Associations with age and memory performance. *Human Brain Mapping, 42*(11), 3620–3642. https://doi.org/10.1002/hbm.25458